Report No. KS-08-6
FINAL REPORT

A TECHNICAL REPORT ON STRUCTURAL EVALUATION OF THE MEADE COUNTY REINFORCED CONCRETE BRIDGE

Asad Esmaeily, Ph.D., P.E.
Kansas State University
Manhattan, Kansas

January 2009

KANSAS DEPARTMENT OF TRANSPORTATION

Division of Operations
Bureau of Materials and Research

KANSAS
DEPARTMENT OF TRANSPORTATION

1 Report No.	2 Government Accession No.	3 Recipient Catalog No.
KS-08-6		

4 Title and Subtitle	5 Report Date
A Technical Report on Structural Evaluation of the Meade County Reinforced Concrete Bridge	January 2009
	6 Performing Organization Code
7 Author(s) Asad Esmaeily, Ph.D., P.E.	8 Performing Organization Report No.
9 Performing Organization Name and Address Kansas State University Civil Engineering Department 2118 Fiedler Hall Manhattan, Kansas 66506	10 Work Unit No. (TRAIS) 11 Contract or Grant No. C1562
12 Sponsoring Agency Name and Address Kansas Department of Transportation Bureau of Materials and Research 700 SW Harrison Street Topeka, Kansas 66603-3745	13 Type of Report and Period Covered Final Report August 2005 - Summer 2008 14 Sponsoring Agency Code RE-0423-01

15 Supplementary Notes
For more information write to address in block 9.

16 Abstract

This is a technical report on the first phase of the evaluation of the Meade County reinforced concrete bridge.

The first three chapters introduce the main problem and provide a general review of the existing evaluation methods and the procedures applicable to the Meade County reinforced concrete bridge.

In chapters four, five and six, the evaluation methods proposed by AASHTO, and ACI, as well as the load rating method using the field crack-test data from the latest bridge inspection conducted in May 2006 and the corresponding results and conclusions are presented.

The report is concluded by chapter seven with the main conclusions and recommendations for the Meade County reinforced concrete bride.

It should be noted that this report serves as the first phase report based on the existing field test data. It is recommended to conduct more tests on the bridge in a near future to cover a wider time-window and provide more field data for a better assessment of the crack propagation, deterioration rate and bridge capacity.

17 Key Words	18 Distribution Statement
reinforced concrete bridge,	No restrictions. This document is available to the public through the National Technical Information Service, Springfield, Virginia 22161

19 Security Classification (of this report)	20 Security Classification (of this page)	21 No. of pages	22 Price
Unclassified	Unclassified	xxx	

Form DOT F 1700.7 (8-72)

A TECHNICAL REPORT ON STRUCTURAL EVALUATION OF THE MEADE COUNTY REINFORCED CONCRETE BRIDGE

Final Report

Prepared by

Asad Esmaeily, Ph.D., P.E.
Kansas State University
Civil Engineering Department
2118 Fiedler Hall
Manhattan, Kansas 66506

A Report on Research Sponsored By

THE KANSAS DEPARTMENT OF TRANSPORTATION
TOPEKA, KANSAS

January 2009

NOTICE

The authors and the state of Kansas do not endorse products or manufacturers. Trade and manufacturers' names appear herein solely because they are considered essential to the object of this report.

This information is available in alternative accessible formats. To obtain an alternative format, contact the Office of Transportation Information, Kansas Department of Transportation, 700 SW Harrison Street, Topeka, Kansas 66603-3745 or phone (785) 296-3585 (Voice) (TDD).

DISCLAIMER

The contents of this report reflect the views of the authors who are responsible for the facts and accuracy of the data presented herein. The contents do not necessarily reflect the views or the policies of the state of Kansas. This report does not constitute a standard, specification or regulation.

ABSTRACT

This is a technical report on the first phase of the evaluation of the Meade County reinforced concrete bridge.

The first three chapters introduce the main problem and provide a general review of the existing evaluation methods and the procedures applicable to the Meade County reinforced concrete bridge.

In chapters four, five and six, the evaluation methods proposed by AASHTO, and ACI, as well as the load rating method using the field crack-test data from the latest bridge inspection conducted in May 2006 and the corresponding results and conclusions are presented.

The report is concluded by chapter seven with the main conclusions and recommendations for the Meade County reinforced concrete bride.

It should be noted that this report serves as the first phase report based on the existing field test data. It is recommended to conduct more tests on the bridge in a near future to cover a wider time-window and provide more field data for a better assessment of the crack propagation, deterioration rate and bridge capacity.

ACKNOWLEDGEMENTS

Hereby the author would like to express his sincere thanks to Mr. Dave Meggers at Kansas Department of Transportation (K-DOT) and acknowledge his valuable help in conducting the field tests and providing the crack-test data, as well as his continuous support, guidance and cooperation.

TABLE OF CONTENTS

CHAPTER 1 - INTRODUCTION

1.1 Problem Statement

Meade County Bridge is a two-lane highway reinforced concrete bridge with two girders each with 20 continuous spans. The bridge was built in 1965. It has been reported that in early years of the bridge service period, a considerable amount of cracks were detected on the bridge girder, with a concentration at the end spans which raised concern on the safety and capacity of the bridge. To address this concern and prevent crack propagation and possible corrosion, the bridge was repaired by epoxy injection and strengthened by rebar insertion in 1986.

In a visual field inspection conducted in June 2004, additional shear cracks were found in Girder “A” of Span 2 at the same location as the cracks in Girder “B”. Shear cracks were also found in both Girders “A” and “B” of Span 27. To provide some means for evaluation of the bridge capacity, field crack tests were conducted using a 54,000 GVM (see Appendix B and Appendix A). The crack pattern and progress, and the crack width and its rate of change under the tested loading have raised concern on the safety of the bridge in general and its existing strength and load capacity, in particular. It should be noted that based on the results from the latest visual inspection of the bridge conducted on May 2006, no further propagation or widening of the cracks and expansion of crack pattern already detected in 2004 was observed. However, the rate of change of the crack-width at some locations under the applied load was slightly more in 2006 compared to 2004, which necessitates more filed data for a better assessment as mentioned in the conclusions. To address the safety concerns, and as an initial and preliminary step towards a thorough evaluation; the existing capacity of the bridge is assessed based on the current conditions as reflected in the visual inspection and field-test data.

1.2 Categories of Evaluation

There are a number of different characteristics or levels of performance of an existing concrete bridge that can be evaluated. These include:

- Stability of the entire bridge
- Stability of individual components of the bridge
- Strength and safety of individual structural elements of the bridge
- The safe load capacity of the bridge
- Stiffness of the entire bridge
- Stiffness of individual structural elements of the bridge
- Susceptibility of individual structural elements of the bridge to excess long-term deformation
- Dynamic response of individual structural elements of the bridge
- Durability of the bridge
- Impact resistance of the bridge
- Serviceability of the bridge

1.3 Objective of the Project

The objective of this technical work was to specify simple analytical methods and use them for prediction of the load capacity of the bridge which in turn can be used to assess the safe load levels for the Meade County reinforced concrete bridge. The current information is limited to the original design and the visual inspection and field crack test data.

It should be noted that methods for evaluation of the other characteristics of an existing concrete bridge need more field test data, and are beyond the scope of this document.

Most bridge evaluations have a number of basic steps in common. However, each evaluation should be treated as unique and emphasis placed on the different steps as dictated by the project. Generally, the evaluation will consist of:

- Defining the existing condition of the bridge, including:
    (1) Reviewing available information on the bridge
    (2) Conducting field observations and condition survey of the bridge
    (3) Determining the cause and rate of progression of existing distress
    (4) Determining the degree of repair to precede the evaluation
- Selecting the bridge elements which require detailed evaluation
- Assessing past, present, and future loading conditions to which the bridge has and will be exposed under the anticipated use
- Conducting the evaluation
- Final report

CHAPTER 2 - PRELIMINARY INVESTIGATION OF THE MEADE COUNTY BRIDGE

Meade County Bridge is a two-lane highway concrete bridge. It has two girders, each with 20 continuous spans. The bridge has been designed based on the design load of H15. The bridge has been built in 1965. During the earlier service stages, many cracks have been detected on the girder body. To prevent crack propagation, the bridge was repaired with epoxy injection and rebar insertion in 1986.

Recently, the bridge was inspected visually and some filed tests were conducted to provide a means to assess the existing conditions of the bridge. The first visual inspection of the bridge was conducted in June 2004. Compared to the early reports, additional shear cracks were found in Girder A of Span 2 at the same location as the cracks in Girder B. The distance from the cracked section to the centerline of the pier is 24.06 ft. Other additional shear cracks were also found in both Girders A and B of Span 27. The crack width was measured and the crack pattern and location was plotted by the inspector. The maximum crack width was 0.19 inches which is larger than the tolerable crack widths normally permitted for reinforced concrete. Crack tests were conducted on Girders A and B using a 54,000 GVM. The distance between the front wheel and the rear wheel was 22’-11’’. The crack width and its rate of change under the loading tests were measured by crack-meters (Vibrating Wire Strain Gages, VWSG, see Appendix C).

The second visual inspection and crack tests on the bridge were conducted in May, 2006. Visual inspection showed that there were no apparent changes in the length, width, and location of the existing cracks inspected in 2004, and no crack propagation was observed. Crack test, identical to those conducted in June 2004, was conducted using crack-meters to measure the crack width and the rate of change under the field test-loads. The rate of change of the crack width was slightly more in 2006 compared to 2004. This issue definitely shows an urgent need for more field tests in time- intervals expanded over a considerable time period to collect enough information for assessment of the rate of deterioration, crack propagation, as well as real capacity of the bridge.

Details of the visual inspection and field test data (in year 2004 and year 2006) can be found in Appendices B and C.

CHAPTER 3 - STRUCTURAL EVALUATION METHODS

3.1 General Description

Deterioration of structures due to aging, cumulative crack growth or excessive response usually decreases structural stiffness and integrity, and therefore significantly affects the structure performance and safety during its service life. Structural Health Monitoring (SHM) denotes the ability to monitor the structure performance and detect and assess such damage at the earliest stage in order to reduce its life-cycle costs and improve its reliability. In this field, Nondestructive Damage Detection (NDD) techniques are employed for continuously monitoring of the structure for possible damage. They are far more convenient and cost effective than traditional methods by testing samples removed from the structure.

The localized NDD methods include acoustic or ultrasonic methods, magnetic field methods, radiograph, microwave/ground penetrating radar, fiber optics, eddy-current methods and thermal field methods. These methods indirectly measure damage by measuring sound, light, electromagnetic field intensity, displacements, or temperature.

The globalized NDD methods include static-based and vibration-based methods. Static-based methods detect damage and evaluate the load capacity, stiffness and stability of the individual or the whole structure by measuring the static displacements and strains on a structure or selected components under load testing; Vibration-based NDD methods detect and assess the changes of the physical properties of a structure by measuring the changes of the vibration characteristics (dynamic properties) of the structure. The vibration-based methods can also be classified into either modal-based or signal-based categories. Modal-based methods use changes in measured modal parameters (resonant frequencies, modal damping, mode shapes, etc.) or their derivatives to present changes in physical-dynamic properties of the structure (stiffness, mass, damping). The basic premise behind the methods is the fact that a change in stiffness leads to a change in natural frequencies and mode shapes. Signal-based methods examine changes in the non-parametric features derived directly from the measured vibration signal through signal processing to detect and assess damage.

3.2 Bridge Evaluation Methods

Bridge evaluation is performed to determine the integrity of the bridge, its deterioration level in terms of the main elements and connections, and load-carrying capacity of all critical elements of the bridge, and the bridge condition as a whole. The ability of the bridge to support all present and anticipated loads according to current code requirements or standards should be considered. Where these code requirements are not met with the bridge in its current condition, appropriate upgrade or strengthening methods and techniques should be determined.

Using the information obtained from the field survey, dimension and geometry evaluation, and material evaluations, the load-carrying capacity of the bridge or portions of the bridge undergoing evaluation should be determined. The choice of the evaluation method is dependent on such factors as the nature of the bridge and the amount of information known about its existing condition. The typical choices are 1) evaluation by analysis, 2) evaluation by load rating, 3) evaluation by non-destructive tests, 4) evaluation by analysis and structural modeling.

Evaluation by analysis: Evaluation by analysis is recommended by ACI when sufficient information is available about the physical characteristics, material properties, structural configuration, and loadings to which the structure has been and will be subjected.

The capacities of the critical components should be determined preferably by the strength design method. Sophisticated methods such as finite element analyses may be used. All existing and expected loads must be considered.

Evaluation by load rating: Evaluation by load rating is recommended by AASHTO. Load rating calculations provide a basis for determining the safe load capacity of a bridge. Load rating requires engineering judgment in determining a rating value that is applicable to maintaining the safe use of the bridge and arriving at posting and permit decisions.

Evaluation by nondestructive load testing: load testing is an effective means of evaluating the structural performance of a bridge or selected components. This applies particularly to those bridges which cannot be accurately modeled by analysis, or to those whose structural response to live load is in question. A load test should only be carried out if the bridge owner believes that it would provide a more realistic appraisal of the load capacity for the bridge. A condition survey and a structural analysis identifying critical components in the bridge should be carried out prior to any load test. Bridge load testing generally consists of load evaluation, diagnostic load testing or proof-load testing. Load evaluation tests are made to determine the magnitude and variation of loads and load effects such as those due to traffic, temperature changes and wind. Diagnostic load tests are performed to determine the effect on various components of a known load on the structure. Proof-load testing is designed to directly determine the maximum live load that the bridge can support safely. The magnitude of the load effect in critical bridge members during the test may exceed the operating level load effects provided the bridge is closed to public during the test.

Evaluation by analysis and structural modeling: If analysis methods can not be used or if adequate facilities are readily available, model testing should be considered. Model testing may be used to advantage when skew or irregularly shaped superstructures are required. The modeling material may be plastic, micro-concrete, or other material which adequately approximates the behavior of the prototype. The effect of scale should be considered.

3.3 Latest Bridge Evaluation Methods Review

Barr et al. (2006) performed live-load test on the San Ysidro Bridge in order to determine changes in deflection, stiffness and load-carrying capacity of the bridge. Externally mounted, bridge diagnostic strain gauges were used to monitor changes in strain that the girders experienced as a load truck was driven across the length of the bridge. Three load paths were chosen to apply the truck load to the bridge. Truck was driven along each of the three load paths at a rate of 5-10 mi. per hour. The slow traveling speed was necessary in order to reduce any dynamic effects of the live load which may be recorded by the strain gages. The strain data was calculated for each of the load paths and girder moments were calculated based on mechanics and design material properties. A full-scale single-lane test was conducted at the laboratory to evaluate the effective shear loads on the bridge. The two load tests in conjunction with finite element modeling were used to determine the load rating for both shear and moment of the bridge. The load rating was then compared with the load rating using the distribution factors from the AASHTO.

Xia and Brownjohn (2004) developed a finite-element model for the quantitative condition assessment of a damaged reinforced concrete bridge deck structure which include damage location and extent, residual stiffness evaluation, and load-carrying capacity assessment. The FE model was validated systematically by correcting uncertainties in the structure based on the dynamically measured data. The moment of inertia of the damaged cross section was identified by using model updating. The relationship between the moment of inertia and the steel ratio of the damaged beam cross section was developed, then the ultimate moment and load-carrying capacity was determined.

Bolton et al. (2005) described the visible damage on the bridge which was severely damaged during the earthquake and the field test procedures were used to determine modal properties (pre-event and post-event modal frequencies, damping, and mode shapes). In the field modal test, an incremental single-input, multiple-output (SIMO), force response test method was used to extract the modal properties of the structure.

Huth et al (2005) investigated the sensitivity of several damage detection-localization, and quantification methods based on modal parameters. Large scale tests with progressive damage on a pre-stressed concrete highway bridge have been performed. During the modal tests, the bridge was excited with a servohydraulic shaker. For estimating modal parameters, the accelerations in three additional locations were measured using accelerometers.

Wang et al (2005) summarized a condition assessment procedure based on a complete system of field-testing, finite element (FE) modeling, and load rating. Experimental techniques, including both model testing and truckload testing were used to collect measurements of the constructed systems. Parameters of FE models were adjusted using both static and dynamic response as criteria to achieve convergence between experimental measurements and analytical results.

3.4 Evaluation Methods for Meade County Bridge

The safety of the Meade County Bridge and also its existing strength and load capacity need to be evaluated based on the visual inspection and the limited field test data available. Although the latest bridge evaluation methods show great potential to evaluate various characteristics of a bridge, including stiffness and strength, they need a lot of static and dynamic testing and also an accurate combined FE model. Based on the current limited information sources on the Meade County Bridge which only include original design and the visual inspection and field crack test data, a thorough review of the existing evaluation methods has shown that AASHTO load rating, ACI truss model and crack test analysis are the reasonable available options that can be selected and applied for the bridge evaluation in this case. These methods provide simple practical steps to evaluate the actual condition of the bridge, in terms of load capacity, strength and safety. These methods can serve as a basis for planning a more detailed study and advanced evaluation procedure to be used for future repairs, rehabilitations and replacements. So, in general, we recommend a more detailed evaluation method based on additional field test data and advanced procedures for better and more realistic and reliable results.

3.4.1 AASHTO Load Rating

Bridge load ratings provide the basis for determining the safe live load capacity of a bridge. The load capacity obtained is used to determine if the bridge has adequate capacity for normal operations. If not, the load rating is used to determine a posting level. In the load rating of bridge members, according to AASHTO specifications, two methods are used for checking the capacity of the members. These methods are allowable stress method and load factor method.

The allowable or working stress method constitutes a traditional specification to provide structural safety. The actual loadings are combined to produce a maximum stress in a member which is not to exceed the allowable or working stress. The latter is found by taking the limiting stress of the material and applying an appropriate factor of safety.

The load factor method is based on analyzing a structure subject to multiples of the actual loads. Different factors are applied to each type of load which reflects the uncertainty inherent in the load calculations. The rating is determined such that the effect of the factored loads does not exceed the strength of the member.

The analytical steps required to rate any member, are independent on the role played by the member in the overall structure. The method of analysis with any of the steps will vary for each member, depending on the member and the choice of Load Factor or Working Stress Method, but the function of the calculations will be the same.

The following analytical steps are required:

1) Determine section properties.
2) Determine allowable and/or yield stresses.
3) Calculate section capacity.
4) Determine dead load effect.
5) Calculate dead load portion of section capacity.
6) Calculate live load effect.
7) Calculate live load impact and distribution.
8) Calculate allowable live load.

For continuous beams, maximum moments, positive or negative due to moving loads can be determined from influence lines, tables (AISC, 1966). In order to simplify analysis, the three-span continuous beam is used to analyze the load capacity instead of twenty-span continuous beam. The lengths of the three spans are 50ft, 72ft and 72 ft, respectively. The influence line tables for three continuous spans are included in the Appendix A. The load capacity on the maximum moment section and the cracking section are evaluated by AASHTO load rating separately and the maximum safe load capacity on the bridge will be controlled by the lower one. The analysis procedures and results are shown in Chapter Four

3.4.2 ACI Truss Model

Truss model calculations provide a basis for determining the shear strength capacity of the bridge section within the crack region. The structural action on the bridge girder can be represented by the truss model, with the main steel providing the tension chord, the concrete top flange acting as the compression chord, the stirrup providing the vertical tension web members, and the concrete between inclined cracks acting as 45^0 compression diagonals.

The tension force in each vertical member represents the force in all the stirrups within a length $jd/\tan\theta$. Similarly, each inclined compression strut represents a width of web equal to $jd\cos\theta$. The uniform load has been idealized as concentrated loads of $w(jd/\tan\theta)$ acting at the panel points.

Such truss model for span 2 in Girder A is built and analyzed by PCA-Frame software. The analysis procedures and results are shown in Chapter Four

3.4.3 Crack Test Analysis

Crack test results show the changes of the crack width on west side, bottom and east side of Girder A and B on Span 2 under three loading conditions. The maximum change of the crack width is on the bottom of Girder B under loading condition 2, rear wheel over the crack (conducted on May, 2006). Such maximum change on the crack section is 0.00707 inch, which was caused by the change of steel tensile strain. The linear elastic relationship between the crack width and the steel tensile stress is assumed in this analysis. Under truck loading condition 2, the steel stress on the cracking section is calculated by using crack width equation with the maximum change of the crack width, 0.00707 inch. The bending moment on this cracking section is calculated by the influence line table (see Appendix A). Then the maximum load capacity is estimated. The analysis procedures and results are shown in Chapter Four

CHAPTER 4 - AASHTO LOAD RATING

4.1 Load Capacity for Maximum Moment Section

The twenty-span continuous bridge girder is simplified as a three-span continuous beam. The lengths of the three spans are 50ft, 72ft and 72 ft. From the influence line table (see Appendix A), the maximum live-load moment (LLM) occurs on the section which is 20 ft (0.4×50=20) away from support on span 1. The maximum load capacity for such three-span continuous beam is controlled by this section. The cross section dimension and property of this section, and also the load rating procedures for this section are shown below.

<u>Condition:</u>

Girder space on 9'-6"

$f_c' = 4000$ psi

$f_c = 1600$ psi

$f_y = 40,000$ psi (unknown)

$f_s = 20,000$ psi

Year built-1965

High density concrete overlay was given in 1985

Current AADT=405

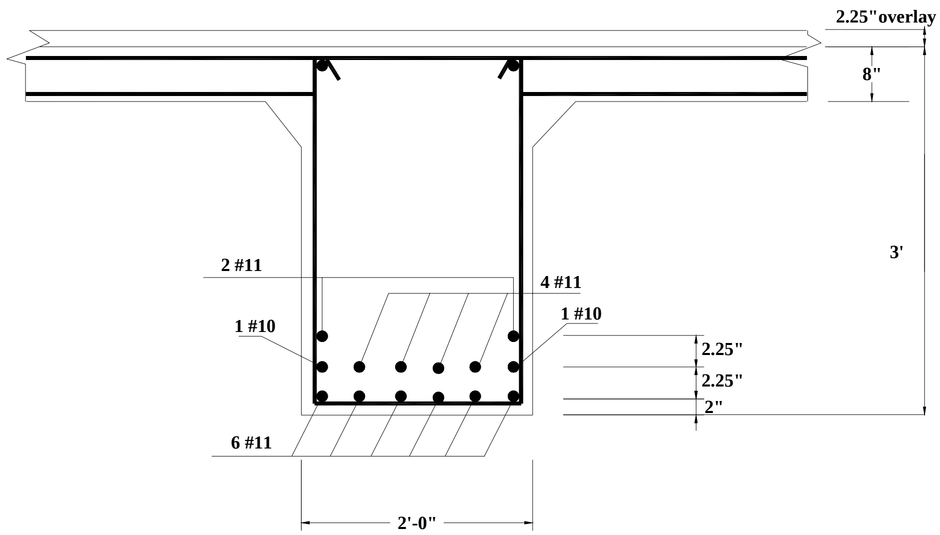

Determine the load

Dead Loads on girder:

The average height of the girder is 5'-8"

Structural Concrete: $0.15\ \text{k/ft}^3 \left[\left(\dfrac{8"}{12"/\text{ft}}\times(10.5+4.2)\right)+\ (2\ \text{ft}\ \times\ 5\ \text{ft}) + 2\left(\dfrac{1}{2}\dfrac{6}{12}\dfrac{6}{12}\right)\right]$

$=3$ k/ft

Concrete Overlay: (2.25 in)

$$0.15\ \text{k/ft}^3 \left[\frac{2.25"}{12"/\text{ft}}\times(9.5'+4.2')\right]=0.40\ \text{k/ft}$$

$$w_{dL}=3+0.40=3.4\ \text{k/ft} \qquad \text{Say } 3.4\ \text{k/ft}$$

Live Load - Rate for H15 vehicle.

Section Properties

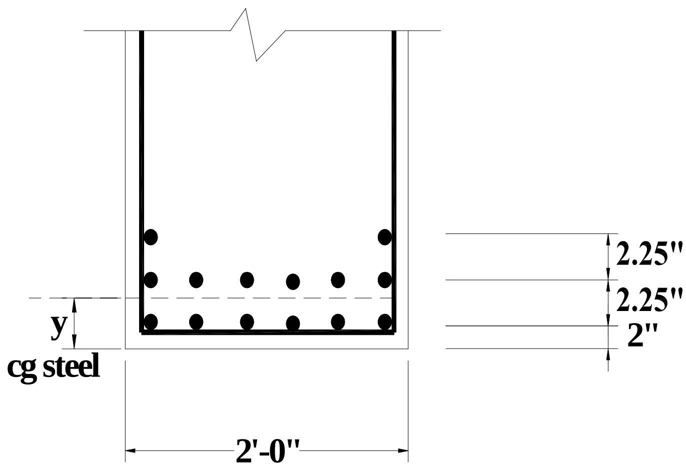

Find cg steel:

$$y=\frac{2(1.27)(2+2.25)+4(1.56)(2+2.25)+6(1.56)(2)+2(1.56)(2+2.25+2.25)}{2(1.27)+12(1.56)}$$

$y=3.59"$

$d_p=2"$

$d=36-3.59=32.41"$

$A_s=12(1.56)+2(1.27)=21.26\ in^2$

$A_s'=4(1.27)=5.08\ in^2$

Effective Slab Width (for T-Girder)

$\frac{1}{4}L=\frac{72\ ft\times12\ in/ft}{4}=216"$

or

CC SPCG =9'-6"=114"

or

$12\ t_s=12\times8=96"$ ÜControls

Cross-Section Moments

Live Load—Rate for H15

The maximum live-load moment (LLM) can be computed from the influence line table (see Appendix A). The maximum live-load moment (LLM) occurs at 20 ft (0.4*50=20) from support on span 1.

The LLM due to one H15 truck is

$M_L = 24(0.2042)(50) + 6(0.0819)(50) = 269.61\text{k - ft}$ (Without impact and without distribution)

The dead load moment:

$$M_d = (0.08)(3.4 \text{ k/ft})(50 \text{ ft})^2 = 680 \text{ k-ft}$$

4.1.1 Allowable Stress Rating

Impact-

AASHTO 3.8.2.1

$$I=\frac{50}{L+125}\text{£}0.30$$

$$I=\frac{50}{50+125}=0.29$$

Distribution –

AASHTO 3.23.2.2 and Table 3.23.1

$$DF=\frac{S_G}{6.0} \quad \text{concrete T-Beam}$$

$$DF=\frac{9.5}{6.0}=1.58$$

Thus the live load moment with impact and distribution

$$M_{L+I}=M_L\left(\frac{1}{2}\right)(1+I)(DF)=269.61\left(\frac{1}{2}\right)(1+0.29)(1.58)=275 \text{ ft-k}$$

Inventory Level

Inventory allowable stress,

$$f_c^I = 0.4f_c^{'} = 0.4(4000) = 1600 \text{ psi} = 1.6 \text{ ksi}$$

For Reinforcing Steel,

$$f_s^I = 20000 \text{ psi} = 20 \text{ ksi}$$

Position of Neutral Axis:

$$k = \sqrt{2\rho n + (\rho n)^2} - \rho n \qquad \text{where: } \rho = \frac{A_s}{bd} = \frac{18.14 \text{ in}^2}{(96 \text{ in})(32.41 \text{ in})}$$

$$k = \sqrt{2(0.0058)(8) + \left[(0.0058)(8)\right]^2} - (0.0058)(8) \qquad \rho = 0.0058$$

$$k = 0.262 \qquad n = \frac{E_s}{E_c} = 8 \text{ (from Article 6.6.2.4)}$$

$$j = 1 - \frac{k}{3} = 1 - \frac{0.262}{3} = 0.91$$

$$kd = (0.262)(32.41) = 8.49" > 8" \text{ the slab thickness}$$

The NA is below bottom of slab and slight into web, but this could be ignored in this case.

Then, capacity if concrete allowable controls-

$$M_c = \frac{1}{2} f_c jkbd^2$$

$$= \frac{1}{2}(1.6 \text{ ksi})(0.91)(0.262)(96 \text{ in})(32.41 \text{ in})^2$$

$$= 19234 \text{ in-k} = 1603 \text{ ft-k}$$

Capacity if steel reinforcement allowable stress controls-

$$M_s = A_s f_s jd$$

$$= \left(21.26\ \text{in}^2\right)\left(20\ \text{ksi}\right)\left(0.91\right)\left(32.41\ \text{in}\right)$$

$$= 12540\ \text{in-k} = 1045\ \text{ft-k}\quad \text{Ü}\text{Controls since } M_s < M_c$$

Rating factor

$$RF_I^A = \frac{M_{RI} - M_D}{M_{L+I}}$$

$$= \frac{1045-680}{275} = 1.33$$

<u>Operating Level:</u>

The operating allowable stress, MANUAL 6.6.2.4 for $f_c^{'} = 4000\text{psi}$

$$f_c^o = 2400\ \text{psi}$$

For Reinforcing Steel, MANUAL 6.6.2.3 controls:

$$f_s^o = 28{,}000\ \text{psi}$$

$$M_s = A_s f_s jd$$
$$= \left(21.26\ \text{in}^2\right)\left(28\ \text{ksi}\right)\left(0.91\right)\left(32.41\ \text{in}\right)$$
$$= 17557\ \text{in-k} = 1463\ \text{ft-k}$$

and checking concrete stress to ensure that concrete does not control

$$f_c = \frac{f_s}{n}\left(\frac{k}{1-k}\right)$$
$$= \left(\frac{28}{8}\right)\left(\frac{0.262}{1-0.262}\right) = 1.24\ \text{ksi} < 2.4\ \text{ksi allowable}$$

Therefore, capacity of section is controlled by allowable steel stress.

Rating factor

$$M_{RO} = 1463 \text{ ft-k}$$
$$\mathrm{RF}_{\mathrm{O}}^{\mathrm{A}} = \frac{M_{RO} - M_D}{M_{L+I}} = \frac{1463 - 680}{275} = 2.85$$

<u>Rate for HS20</u>

Live Load

Rate for HS20 truck load

$M_L = 8(0.0494)(50) + 32(0.2042)(50) + 32(0.0819)(50) = 477.52$ k-ft (Without impact and without distribution)

$M_{L+I} = M_L(1+I)(\frac{1}{2})(DF) = 477.52(\frac{1}{2})(1+0.29)(1.58) = 487$ ft-k

<u>Inventory Level</u>

Rate factor

$$RF_I^A = \frac{M_{RI} - M_D}{M_{L+I}}$$
$$= \frac{1045-680}{487} = 0.75$$

<u>Operating Level:</u>

Rate factor

$$RF_O^A = \frac{M_{RO} - M_D}{M_{L+I}} = \frac{1463-680}{487} = 1.61$$

Load Capacity Based on Allowable Stress Method

Inventory: $1.33 \times 15^{T} = 20^{T}$ H15

Operating: $2.85 \times 15^{T} = 42.8^{T}$ H15

Inventory: $0.75 \times 36^{T} = 27^{T}$ HS20

Operating: $1.61 \times 36^{T} = 58^{T}$ HS20

4.1.2 Load Factor Rating

Live Load

Rate for H15 truck load

Impact-

AASHTO 3.8.2.1

$$\mathrm{I} = \frac{50}{\mathrm{L} + 125} \le 0.30$$

$$\mathrm{I} = \frac{50}{50 + 125} = 0.29$$

Distribution –

AASHTO 3.23.2.2 and Table 3.23.1

$$\mathrm{DF} = \frac{\mathrm{S_G}}{6.0} \text{ concrete T-Beam}$$

$$\mathrm{DF} = \frac{9.5}{6.0} = 1.58$$

Thus the live load moment with impact and distribution

$$M_{L+I} = M_L\left(\frac{1}{2}\right)(1+I)(DF) = 269.61\left(\frac{1}{2}\right)(1+0.29)(1.58) = 275 \text{ ft-k}$$

Capacity of section:

$$A_s = 12(1.56) + 2(1.27) = 21.26 \text{ in}^2$$

$$A_s' = 4(1.27) = 5.08 \text{ in}^2$$

$$f_y = 40 \text{ ksi} \qquad f_c' = 40000 \text{ psi}$$

$$d = 32.41 \text{ in} \qquad b_w = 24 \text{ in}$$

$$h = 36 \text{ in} \qquad b_{eff} = 12h_f = 12(8) = 96 \text{ in}$$

$$a = \frac{A_s f_y}{0.85 f_c' b_{eff}} = \frac{21.26(40)}{0.85(4)(96)} = 2.61 \text{ in} < 8 \text{ in OK within slab}$$

$$M_R = A_s f_y \left(d - \frac{a}{2}\right) = 21.26(40)\left(32.41 - \frac{2.61}{2}\right) = 26452 \text{ k-in} = 2204 \text{ k-ft}$$

$$M_u = jM_R$$

$$M_u = 0.9 \times 2204 = 1984 \text{ k-ft}$$

Inventory Level: MANUAL 6.5.1 & 6.6.3

Rate factor

$$R_I^{LF} = \frac{M_u - A_1 M_D}{A_2 M_{L+I}}$$

where in accordance with MANUAL 6.5.3

$$A_1 = 1.3$$

$$A_2 = 2.17$$

Thus:

$$RF_I^{LF} = \frac{1984 - 1.3(680)}{2.17(275)} = 1.84$$

Operating Level: MANUAL 6.5.1 & 6.6.3

Rate factor

$$R_O^{LF} = \frac{M_u - A_1 M_D}{A_2 M_{L+I}}$$

where in accordance with MANUAL 6.5.3

$$\gamma_D = 1.3$$
$$\gamma_L = 1.3$$

Thus:

$$RF_O^{LF} = \frac{1984 - 1.3(680)}{1.3(275)} = 3.08$$

Rate for HS20

Live Load—Rate for HS20

$$M_{L+I} = 487 \text{ k-ft}$$

Inventory Level:

Rate factor

$$RF_I^{LF} = \frac{1984 - 1.3(680)}{2.17(487)} = 1.04$$

Operating Level:

Rate factor

$$RF_O^{LF} = \frac{1984 - 1.3(680)}{1.3(487)} = 1.74$$

Load capacity based on Load Factor Method

$$\text{Inventory}: 1.84 \times 15^T = 27.6^T \ \ \text{H15}$$

$$\text{Operating}: 3.08 \times 15^T = 46.2^T \ \text{H15}$$

$$\text{Inventory}: 1.04 \times 36^T = 37.4^T \ \text{HS20}$$

$$\text{Operating}: 1.74 \times 36^T = 62.6^T \ \text{HS20}$$

Summary the results

Load capacity for the maximum moment section

Method	H Truck Max. Load (tons)	HS Truck Max. Load (tons)
Allowable Stress:		
Inventory	20	27
Operating	42.8	58
Load Factor		
Inventory	27.6	37.4
Operating	46.2	62.6

4.2 Load Capacity for Cracked Section

The cracking happened on span 2. The length of span 2 is 72 ft. The original cross-section at the cracking location is shown below. The distance from the crack location to the centerline of the column is 24.07’ (23.4 ‘+ 8” =24.07’). The procedures for load rating on this cracking section are also shown below.

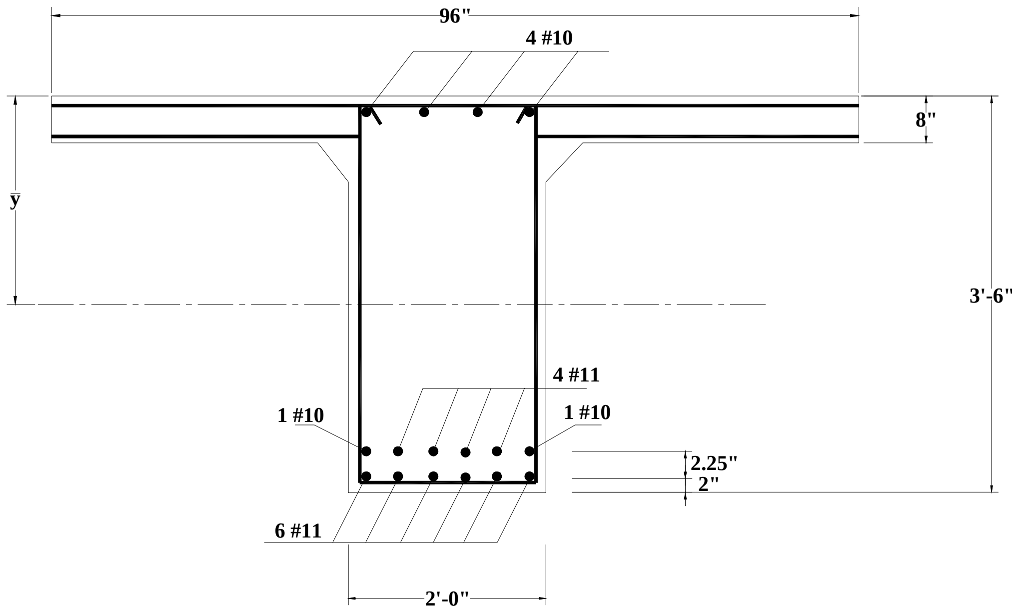

Section Properties

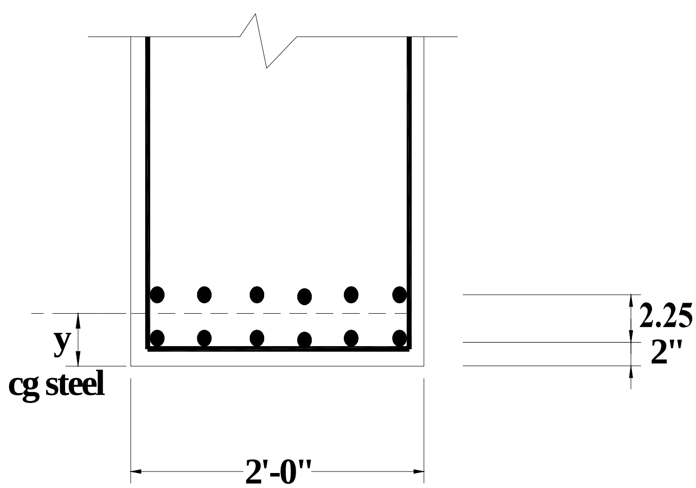

Find cg steel:

$$y=\frac{2(1.27)(2+2.25)+4(1.56)(2+2.25)+6(1.56)(2)}{2(1.27)+10(1.56)}$$

$$y=3.09"$$

$$d_p=2"$$

$$d=42-3.09=38.91"$$

$$A_s=10(1.56)+2(1.27)=18.14\ in^2$$

$$A_s^{'}=4(1.27)=5.08\ in^2$$

Effective Slab Width (for T-Girder)

$$\frac{1}{4}L=\frac{72\ ft\times 12\ in/ft}{4}=216"$$

or

$$CC\ SPCG=9'-6"=114"$$

or

$$12\ t_s=12\times 8=96"\ \text{Ü}\ \text{Controls}$$

Cross-Section Moments at Cracking Location

Live Load—Rate for H15

The maximum live-load moment (LLM) at cracking location can be computed from the influence line table (see Appendix C). The LLM due to one H15 truck is

$$M_L=24(0.1414)(50)+6(0.075)(50)=192.18\ k-ft$$

(Without impact and without distribution)

The dead load moment at cracking location:

$$M_d=(0.0050)(3.4\ k/ft)(50\ ft)^2=42.5\ k-ft$$

4.2.1 Allowable Stress Rating

Impact-

AASHTO 3.8.2.1

$$I = \frac{50}{L + 125} \le 0.30$$

$$I = \frac{50}{50 + 125} = 0.29$$

Distribution –

AASHTO 3.23.2.2 and Table 3.23.1

$$DF = \frac{S_G}{6.0} \text{ concrete T-Beam}$$

$$DF = \frac{9.5}{6.0} = 1.58$$

Thus: the live load moment with impact and distribution

$$M_{L+I} = M_L\left(1 + I\right)\left(\frac{1}{2}\right)\left(DF\right) = 192.18\left(1 + 0.29\right)\left(\frac{1}{2}\right)\left(1.58\right) = 196 \text{ ft-k}$$

Inventory Level

Capacity of steel reinforcement allowable stress after crack

After cracking:

centroid of cracked transformed section, $\bar{y}$

$$72\times 8\times\left(\bar{y}-4\right)+\frac{\bar{y}^2}{2}b+A_s^{'}\times\left(n-1\right)\left(\bar{y}-2\right)-A_s n\left(d-\bar{y}\right)=0$$

$$576\times\left(\bar{y}-4\right)+\frac{\bar{y}^2}{2}\times 24+5.08\times 7\times\left(\bar{y}-2\right)-18.14\times 8\times\left(38.91-d\right)=0$$

$$\Rightarrow \bar{y}=9.25\text{ in}$$

$$M_s=f_s A_s\left(d-\frac{\bar{y}}{2}\right)=\left(20\text{ksi}\right)\left(18.14\text{in}^2\right)\left(38.91-\frac{9.25}{2}\right)$$

$$=12439\text{ in-k}=1036\text{ ft-k}$$

$$RF_I^A=\frac{MR_I-M_D}{M_{L+I}}=\frac{1036-42.5}{196}=5.06$$

<u>Operating Level: MANUAL 6.5.2 & 6.6.2.4</u>

The operating allowable stress, MANUAL 6.6.2.3 for reinforcing steel $f_s^o=28\text{ ksi}$

Thus:

$$M_s=f_s A_s\left(d-\frac{\bar{y}}{2}\right)=\left(28\text{ksi}\right)\left(18.14\text{in}^2\right)\left(38.91-\frac{9.25}{2}\right)$$

$$=17414\text{ in-k}=1451\text{ ft-k}$$

Therefore, $M_{RO}=1451\text{ ft-k}$

Rate factor

$$RF_O^A=\frac{MR_{RO}-M_D}{M_{L+I}}=\frac{1451-42.5}{196}=7.2$$

Rate for HS20

Live Load

---Rate for HS20 truck load

Live load moment without impact and distribution

$$M_L = 8(0.0572)(50) + 32(0.1414)(50) + 32(0.0655)(50) = 353.92\,\text{k-ft}$$

The dead load moment at cracking location

$$M_d = 42.5\,\text{k-ft}$$

$$M_{L+I} = M_L\,(1+I)(\frac{1}{2})(DF) = 353.92(1+0.29)(\frac{1}{2})(1.58) = 361\,\text{ft-k}$$

Inventory Level

Rate factor

$$RF_I^A = \frac{MR_I - M_D}{M_{L+I}} = \frac{1036 - 42.5}{361} = 2.75$$

Operating Level:

$$RF_O^A = \frac{MR_{RO} - M_D}{M_{L+I}} = \frac{1451 - 42.5}{361} = 3.9$$

Load Capacity Based on Allowable Stress Method

$$\text{Inventory}: 5.06 \times 15^T = 76^T \ \text{H15}$$

$$\text{Operating}: 7.2 \times 15^T = 108^T\ \text{H15}$$

$$\text{Inventory}: 2.75 \times 36^T = 99^T\ \text{HS20}$$

$$\text{Operating}: 3.9 \times 36^T = 140^T\ \text{HS20}$$

4.2.2 Load Factor Rating

$$M_R = f_y A_s \left(d - \frac{\bar{y}}{2} \right) = (40\text{ksi})(18.14\text{in}^2)\left(38.91 - \frac{9.25}{2}\right)$$

$$= 24877 \text{ in-k} = 2073 \text{ ft-k}$$

$$M_u = jM_R$$

$$M_u = 0.9(2073) = 1866 \text{ k-ft}$$

Rate for H15

Inventory Level: MANUAL 6.5.1 & 6.6.3

$$R_I^{LF} = \frac{M_u - A_1 M_D}{A_2 M_{L+I}}$$

where in accordance with MANUAL 6.5.3

$$A_1 = 1.3$$

$$A_2 = 2.17$$

Thus:

$$RF_I^{LF} = \frac{1866 - 1.3(42.5)}{2.17(196)} = 4.25$$

Operating Level: MANUAL 6.5.1 & 6.6.3

$$R_O^{LF} = \frac{M_u - A_1 M_D}{A_2 M_{L+I}}$$

where in accordance with MANUAL 6.5.3

$$\gamma_D = 1.3$$

$$\gamma_L = 1.3$$

Thus:

$$RF_O^{LF} = \frac{1866 - 1.3(42.5)}{1.3(196)} = 7.1$$

Rate for HS20

Live Load—Rate for HS20

For H20

$$M_{L+I} = 361\,\text{ft-k}$$

Inventory Level:

$$RF_I^{LF} = \frac{1866 - 1.3(42.5)}{2.17(361)} = 2.3$$

Operating Level:

$$RF_O^{LF} = \frac{1866 - 1.3(42.5)}{1.3(361)} = 3.86$$

Load capacity based on Load Factor Method

$$\text{Inventory}: 4.25 \times 15^T = 64^T \ \text{H15}$$

$$\text{Operating}: 7.1 \times 15^T = 107^T \ \text{H15}$$

$$\text{Inventory}: 2.3 \times 36^T = 83^T \ \text{HS20}$$

$$\text{Operating}: 3.86 \times 36^T = 139^T \ \text{HS20}$$

<u>Summary the results</u>

Load capacity for the cracked section

Method	H Truck Max. Load (tons)	HS Truck Max. Load (tons)
Allowable Stress:		
Inventory	76	99
Operating	108	140
Load Factor		
Inventory	64	83
Operating	107	139

4.3 Conclusion

AASHTO load rating shows that the load capacity for the cracked section is much higher than that for the maximum moment section. Therefore, so far, the maximum load on the whole bridge should be controlled by the load capacity for the maximum moment section, as repeated in the following table.

Method	H Truck Max. Load (tons)	HS Truck Max. Load (tons)
Allowable Stress:		
Inventory	20	27
Operating	42.8	58
Load Factor		
Inventory	27.6	37.4
Operating	46.2	62.6

CHAPTER 5 - TRUSS MODEL

5.1 General Procedure

The structural action of the bridge girder can be represented by the truss model, with the main steel providing the tension chord, the concrete top flange acting as the compression chord, the stirrup providing the vertical tension web members, and the concrete between inclined cracks acting as 45^0 compression diagonals.

The tension force in each vertical member represents the force in all the stirrups within a length $jd / tan\theta$. Similarly, each inclined compression strut represents a width of web equal to $jd\, cos\theta$.The uniform load has been idealized as concentrated loads of $w(jd / tan\theta)$ acting at the panel points. The following figure shows such a truss model. There are totally 61 members included in this model. The length for any vertical members is 5ft; the length for any horizontal member except member 2 and 60, is 5ft; the length for each of member 2 and 60 is 2.5ft.

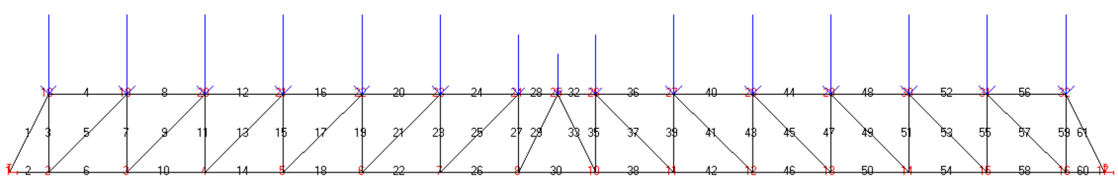

Loading condition

To be on the conservative safe side, the truck load used here is HS20

$\text{Dead load}: 3.4\ \text{k}/\text{ft}$

$\text{Live load}: 0.64\ \text{k}$(stand HS lane load with uniform load 640 lbs per linear foot of load lane)

$w = 1.2(3.4) + 1.6(0.64) = 5\ \text{kip}/\text{ft}$

point load applied on truss model:

$P = wjd/\tan\theta$

$jd = 5' \quad \theta = 45^0$

$\text{so } P = 5(5) = 25\text{kip}$

Truss member 18 represents the longitudinal reinforcement steel which is within the inclined crack region.

Horizontal force F_x = 72.2 kips

A_s = 18.14 in^2 f_s =72.2/18.14=3.98 ksi

Check the crushing strength of concrete in the web

The web of the beam will crush if the inclined compressive stress exceeds the strength of the concrete. Truss member 17 represents the inclined compression within the crack region. The following PCA outputs show the internal force for member 17.

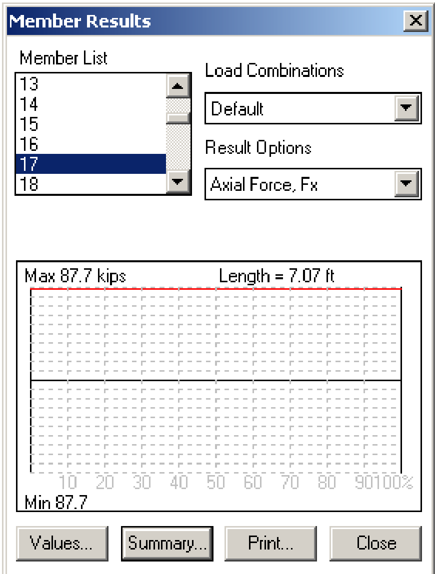

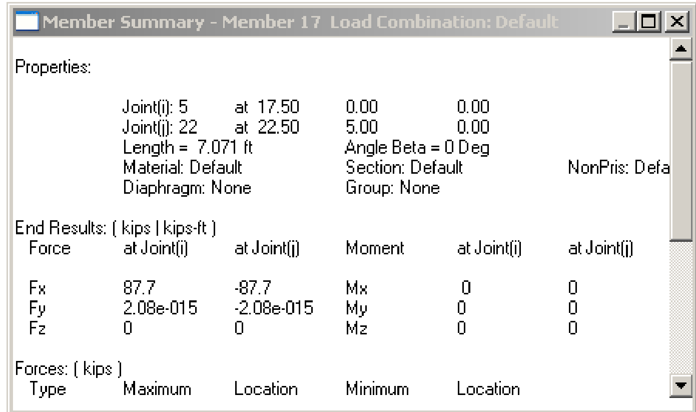

$$D = 87.7 \text{ kips}$$

$$f_{cd} = \frac{D}{b_w jd\cos\theta} = \frac{87.7}{24(12)(5)\cos 45^0} = 0.1\text{ksi} < \text{f}_\text{c} = 1.6\text{ksi}$$

<u>OK</u>

<u>Check stirrups at the inclined crack.</u>

Truss member 19 represents the stirrup within the cracked region. The following PCA outputs show the internal force for member 19.

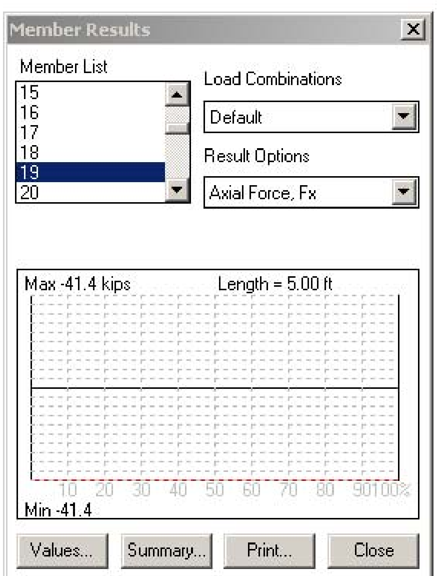

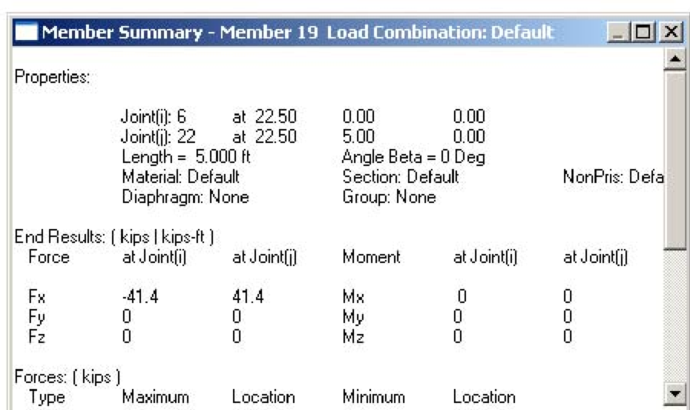

From the output: $V_u = 41.4 \text{ kips}$,

The existing stirrup-spacing within the cracked region is 2 feet ($s = 2\,ft = 24in$)

$$A_v f_y = \frac{\frac{V_u}{j} s}{jd / \tan\theta} = \frac{\frac{41.4}{0.75}(24)}{5(12)} = 22.08\text{kip}$$

$$A_v = \frac{22.08}{40} = 0.552\,\text{in}^2 \text{ (the required steel area for this spacing based on demanded load)}$$

As mentioned, the No.4 stirrup@2 ft is provided within the cracked region.

$$A_v = 0.2(2) = 0.4\,\text{in}^2 \text{ (provided)} < A_v = 0.552 \text{ (Required area per demanded load)}$$

So, the shear reinforcement provided when the bridge was designed is not enough for the design load.

<u>Minimum Web Reinforcement Requirements:</u>

AASHTO minimum web reinforcement requirement

$$A_v = \sqrt{f_c^{'}}\, b_v s / f_y = \sqrt{4000}(24)(24)/40{,}000 = 0.91\text{in}^2,$$

and specifies maximum spacing of transverse reinforcement of $s \le 0.8d_v \le 24 \text{ in}$, when $v_u \le 0.125 f_c^{'}$

So, per AASHTO, the minimum area for the existing spacing is 0.91 in^2, and the minimum spacing is less than 24 in.

ACI minimum web reinforcement requirement

$$A_v = 0.75\sqrt{f_c^{'}}\frac{b_w s}{f_y} \geq 50\frac{b_w s}{f_y} = 50\frac{24(24)}{40,000} = 0.72$$

$$= 0.75\sqrt{4000}\frac{24(24)}{40,000}$$

$$= 0.68$$

so the minimum area of web reinforcement based on ACI is equal to 0.72 in^2

ACI maximum stirrup spacing requirement

For the cracking section:

$$b_w = 24 \text{ in}$$

$$h = 3'\text{-}6'' = 42 \text{ in}$$

$$\text{cg steel}: y = 3.09 \text{ in}$$

$$d = 42 - 3.09 = 38.91 \text{ in}$$

$$f_c^{'} = 4000 \text{ psi}$$

$$s_{max} = \min\{24 \text{ in or } d/2\} = \frac{d}{2} = \frac{38.91}{2}$$

$$= 20 \text{ in } (V_s < 4\sqrt{f_c^{'}}b_w d$$

$$= 4\sqrt{4000}(24)(38.91)$$

$$= 236 \text{ kips})$$

The current stirrup spacing on the crack section (s= 24 in) exceeds the ACI specified maximum stirrup spacing (s_{max} = 20 in).

5.2 Conclusion

Under HS20 truck lane load, the inclined demanded compressive stress in the web of the beam is less than the strength provided by concrete, however, the demanded vertical shear force on the cracked section is more than the strength provided by No.4 stirrup@2 ft. It should be noted that the load has been factored by the load factors and the strength reduced by the current strength reduction factor per the AASHTO as well as ACI code. If the load factors and strength reduction factor are not applied, the exact value of the calculated strength will slightly be more than the demanded values for HS20 truck load. Also, the amount of stirrups crossing the cracked region is slightly less than the minimum amount of the web reinforcement required by AASHTO and ACI for the existing spacing and the spacing is less than the maximum limit required by the ACI and AASHTO. The minimum current stirrup spacing within the cracked section (s= 24 in) exceeds the ACI specified maximum stirrup spacing requirement (s_{max} = 20 in). This means that when the bridge was designed, this requirement has been overlooked.

CHAPTER 6 - CRACK TEST ANALYSIS

Crack tests are conducted by using 54,000 GVM. The axle distance between the front wheel and the far rear wheel is 22'-11". The weight on the front axle is 20,000 pounds, and the weight on the rear two-axle is 17,000 pounds per each. The maximum change of the crack width was observed on the bottom of Girder B under loading condition 2, when rear wheel was over the crack (conducted on May, 2006). This maximum change of the crack width was 0.00707 inch, caused by the induced change in the steel strain under the applied load. In reinforced concrete analysis procedures, sections with conventional reinforcement are considered to be linear and elastic beyond the cracking load level, usually up to the first yield of the tensile steel. So, in this analysis it has been assumed that the relationship between the crack width and the steel strain and in turn the applied load is linear. Under truck loading condition 2, the steel stress on the cracked section is calculated by using crack width equation, proposed by Frosch (B. B. Broms, 1965) with the maximum change of the crack width, 0.00707 inch. The bending moment on this cracked section is calculated by the influence line table (see Appendix A). The figure below shows the crack test under condition 2, "rear wheel over the crack".

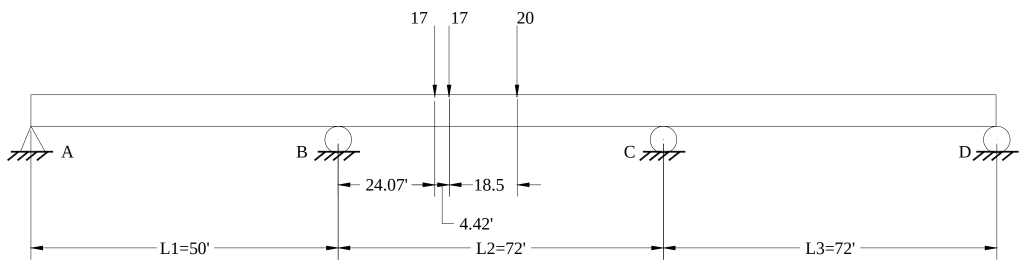

$$w = 2000\frac{f_s}{E_s}\beta\sqrt{d_c^{\,2} + \left(\frac{s}{2}\right)^2} \qquad \text{(Frosch Equation)}$$

$$d_c = 3"$$

$$s = 4"$$

$$E_s = 29000\text{ksi}$$

$$w = 7.07 \text{ (in unit of 0.001in.)}$$

$$7.07 = 2000\frac{f_s}{29000}(1.20)\sqrt{3^2 + \left(\frac{4}{2}\right)^2}$$

$$\Rightarrow f_s = 23.7 \text{ ksi}$$

Load capacity on the section with cracking

Allowable Stress Rating

$$M_L = 0.1414(17)(50) + 0.1048(17)(50) + 0.0419(20)(50)$$

$$= 251.17 \text{ k-ft}$$

$$M_{L+I} = 251.17(1+0.29)\left(\frac{1}{2}\right)(1.58) = 256 \text{ k-ft}$$

Rate for H15 truck

Inventory Level

Inventory allowable stress for Reinforcing Steel,

$$f_s^I = 20000 \text{ psi} = 20 \text{ ksi}$$

$$\text{when } f_s = 23.7 \text{ ksi} \Rightarrow M = 256 \text{ k-ft}$$

$$f_s = 20 \text{ ksi} \Rightarrow M_{RI} = ?$$

$$\frac{23.7}{256} = \frac{f_s = 20}{M_{RI}} \qquad \Rightarrow M_{RI} = 216 \text{ k-ft}$$

$M_{L+I} = 196$ ft-k (See Chapter 4.2.1 Allowable Stress Rating for H15)

$$RF_I^A = \frac{M_{RI} - M_D}{M_{L+I}}$$

$$= \frac{216 - 42.5}{196} = 0.88$$

Operating Level:

For Reinforcing Steel, MANUAL 6.6.2.3

$$f_s^o = 28,000 \text{ psi}$$

$$\text{when } f_s = 23.7 \text{ ksi} \Rightarrow M = 256 \text{ k-ft}$$

$$f_s = 28 \text{ ksi} \Rightarrow M_{RO} = ?$$

$$\frac{23.7}{256} = \frac{f_s = 28}{M_{RO}} \qquad \Rightarrow M_{RO} = 302 \text{ k-ft}$$

$$RF_O^A = \frac{M_{RO} - M_D}{M_{L+I}} = \frac{302 - 42.5}{196} = 1.3$$

<u>Rate for HS20 truck</u>

<u>Inventory Level</u>

$M_{L+I} = 361 \text{ ft-k}$ (See Chapter 4.2.1, rate for HS20)

$$RF_I^A = \frac{M_{RI} - M_D}{M_{L+I}}$$

$$= \frac{216 - 42.5}{361} = 0.48$$

<u>Operating Level</u>

$$RF_O^A = \frac{M_{RO} - M_D}{M_{L+I}} = \frac{302 - 42.5}{361} = 0.72$$

Local Capacity Based on Allowable Stress

Inventory:	$0.88 \times 15^T = 13.2^T$	H15
Operating:	$1.3 \times 15^T = 20^T$	H15
Inventory:	$0.48 \times 36^T = 17^T$	HS20
Operating:	$0.72 \times 36^T = 26^T$	HS20

Load Factor Rating

$$\text{when } f_s = 23.7 \text{ ksi } \Rightarrow M = 256 \text{ k-ft}$$

$$f_s = f_y = 40 \text{ ksi } \Rightarrow M_R = ?$$

$$\frac{23.7}{256} = \frac{f_y = 40}{M_R} \qquad \Rightarrow M_R = 432 \text{ k-ft}$$

$$M_u = \varphi M_R$$

$$M_u = 0.9\left(432\right) = 389 \text{ k-ft}$$

Rate for H15

Inventory Level: MANUAL 6.5.1 & 6.6.3

$$R_I^{LF} = \frac{M_u - A_1 M_D}{A_2 M_{L+I}}$$

where in accordance with MANUAL 6.5.3

$$A_1 = 1.3$$

$$A_2 = 2.17$$

Thus:

$$RF_I^{LF} = \frac{389 - 1.3\left(42.5\right)}{2.17\left(196\right)} = 0.78$$

Operating Level: MANUAL 6.5.1 & 6.6.3

$$R_O^{LF} = \frac{M_u - A_1 M_D}{A_2 M_{L+I}}$$

where in accordance with MANUAL 6.5.3

$$\gamma_D = 1.3$$

$$\gamma_L = 1.3$$

Thus:

$$RF_O^{LF} = \frac{389 - 1.3(42.5)}{1.3(196)} = 1.3$$

Rate for HS20

Live Load—Rate for HS20

For H20

$$M_{L+I} = 361 \text{ ft-k}$$

Inventory Level:

$$RF_I^{LF} = \frac{389 - 1.3(42.5)}{2.17(361)} = 0.43$$

Operating Level:

$$RF_O^{LF} = \frac{389 - 1.3(42.5)}{1.3(361)} = 0.71$$

Local Capacity Based on Allowable Stress

$$\text{Inventory}: \quad 0.78 \times 15^T = 12^T \qquad \text{H15}$$

$$\text{Operating}: \quad 1.3 \times 15^T = 20^T \qquad \text{H15}$$

$$\text{Inventory}: \quad 0.43 \times 36^T = 15.5^T \qquad \text{HS20}$$

$$\text{Operating}: \quad 0.71 \times 36^T = 26^T \qquad \text{HS20}$$

Load capacity based on Crack Test Analysis

Method	H Truck Max. Load (tons)	HS Truck Max. Load (tons)
Allowable Stress:		
Inventory	13	17
Operating	20	26
Load Factor		
Inventory	12	15.5
Operating	20	26

The load capacity of the cracked section is re-evaluated by using the crack test results. The load capacity of the cracked section rated by crack test analysis is significantly lower than the load capacity for the maximum moment section rated by AASHTO method. So, conservatively, it is recommended to limit the maximum level of the bridge load to the values in the table above.

CHAPTER 7 - CONCLUSION AND RECOMMENDATION

Meade County Bridge is a two-lane highway concrete bridge. The design load of the bridge has been H15. The recent visual inspections and crack tests on the bridge were conducted in June1, 2004 and May 2006. Compared to earlier inspections, the inspection in 2004 showed additional shear cracks on Girder A of Span 2 at the same location as the cracks on Girder B. The latest visual inspection and crack tests conducted in May, 2006, did not show a significant change in the crack pattern, width, or propagation; however, the rate of change of the crack width at some locations was slightly more compared to 2004. This is a concern that needs to be addressed. Three structural evaluation methods were used to estimate the maximum load-carrying capacity of the bridge. The evaluation procedure was conducted by application of the pertinent methods to a number of critical sections, namely the section with the maximum demanded bending moment and the section with critical shear strength at the cracked region.

7.1 Conclusions

The load capacities of the maximum moment section and the cracked section were evaluated by AASHTO load rating method, separately. The load capacity of the maximum moment section was lower than the load capacity of the cracked section.

The cracks on the girder are mostly shear cracks generated by shear force. The shear strength at the cracked section was evaluated by truss model. Under HS20 truck lane load (which is higher than the design load of the bridge), the inclined demanded compressive stress in the web of the beam was less than the strength provided by the concrete. The demanded vertical shear force at the cracked section was slightly more than the resistance provided by No.4 stirrup@2 ft, when the loads are increased by the load factors and the strength is reduced by the strength reduction factor, which is 0.75 based on the current code. Also, the amount of stirrups crossing the cracked section is slightly less than the minimum amount of the web reinforcement required by AASHTO and ACI, and the spacing is larger than the maximum value dictated by AASHTO and ACI code. So, while the exact value of the demanded shear is slightly less than the shear strength provided by the shear steel, the demanded shear using factored loads is larger than the strength provided by the shear steel reduced by the strength reduction factor.

The load capacity of the cracked section was re-evaluated using the crack test data. The load capacity of the cracked section, rated by crack test analysis, was significantly lower than the load capacity of the maximum moment section, as the controlling section, rated by the method recommended by AASHTO. So, the load capacity for the whole bridge is controlled by the load capacity of the cracked section and the values evaluated by the field test data will control the maximum level of the load applicable to the bridge, and should conservatively be considered for this bridge, as shown in the following table.

It can be concluded that under the design load of HS15, and considering the fact that no change has been observed during the course of the two years between the two successive inspections (June 2004 to May 2006) in terms of crack propagation, widening of the existing cracks or change in their pattern, except for a slight increase in the rate of change of the crack width at a few locations; the bridge can remain open but the loading of the bridge should be closely monitored and the maximum level of load should be limited to the values in this table. However, this limitation is on the conservative side until more detailed and accurate field test-data is available and a comprehensive analysis is conducted for a better, accurate and realistic evaluation of the bridge condition and assessment of the maximum safe load level.

Load capacity for the bridge

Method	H Truck Max. Load (tons)	HS Truck Max. Load (tons)
Allowable Stress:		
Inventory	13	17
Operating	20	26
Load Factor		
Inventory	12	15.5
Operating	20	26

7.2 Recommendations

The latest visual inspection and crack tests on the bridge were conducted in May, 2006. Visual inspection shows that there are no changes in length, width, propagation and location of the existing cracks inspected in 2004. The crack tests show that the rate of change of the crack width on the bottom of the cracked section under the test-load in 2006, used in the analysis, is slightly higher than the corresponding values measured in 2004. This issue definitely shows an urgent need for more field tests in time-intervals expanded over a considerable time period to collect enough information for assessment of the rate of deterioration, crack propagation, as well as real capacity of the bridge.

When the load capacity of the bridge is rated based on the load test analysis, the higher rate of change of the crack-width on the bottom of the cracked section leads to a considerable decrease in the load capacity of the bridge.

The main recommendations can be summarized as follows:

1. Based on the existing information and the field tests conducted in 2004 and especially in 2006, it is recommended to closely and continuously monitor the bridge and keep the maximum level of the loading limited to the values as in the table above.
2. The limitation as stated above is on the conservative side, considering the performance of the bridge during the past two years. So, if a record of the loading history of the bridge during the past 2 years is available, the limit can be increased to the maximum levels used during this period, under urgent cases, however, this is not conservative and the limitation is required for normal daily use of the bridge, until more detailed field test are conducted and the bridge condition is re-evaluated using more advanced methods and procedures for an accurate assessment of the existing capacity and safe-load levels, and recommendation of the best retrofit, repair or replacement method
3. Conventional repair and strengthening methods, such as epoxy injection and rebar insertion based on a carefully studied plan should be practiced to elevate the safety level of the bridge; before a general repair (or replacement) procedure can be recommended based on the aforesaid detailed and advanced study on the bridge condition
4. Continuous monitoring of the bridge and more frequent inspection is strongly recommended. It is better to implement an automated continuous monitoring system that can provide a complete record of the loading

history, local deformations, deflections and strains at pre-defined locations and the corresponding peak values experienced by the bridge during the monitored time window. This will provide a valuable source of data that can be used for a better realistic assessment of the bride, which can in turn, be used to find the optimal repair, retrofit or replacement scenario.

5. A more comprehensive study of the bridge, including field test and evaluation methods and procedures is recommended for a more accurate and realistic analysis of the bridge condition, assessment of the bridge safety and capacity, and proposing the optimal process to address the deficiencies. The recommended study, while for this bridge, will provide a valuable resource to evaluate other bridges with identical or similar conditions. The results can be expanded later to provide an optimal system and the pertinent algorithm for an efficient health monitoring of bridges.

REFERENCES

AASHTO(1994). “Manual for Condition Evaluation of Bridges” AASHTO, Washington, D.C

ACI 343R-95 (1995). “Analysis and Design of Reinforced Concrete Bridge Structures” ACI

ACI 437R-91 (1997). ”Strength Evaluation of Existing Concrete Buildings” ACI

ACI 364.1 R-94 (1999). ”Guide for Evaluation of Concrete Structures prior to Rehabilitation” ACI

AISC (1966). “Moments, shear, and reactions for continuous highway bridge” AISC, Chicago.

Barker, R.M., and Puckett, J.A., (1997).”Design of Highway Bridge: based on AASHTO LRFD bridge design specification.” John Wiley, New York.

B. B. Broms, “Crack Width and Crack Spacing in Reinforced Concrete Members”, J. ACI, vol 62, No. 10, 1965, pp 1237-1256

Barr, P.J., Woodward, C.B., Najera, B., and Amin, M. N., (2006). “Long-term structural health monitoring of the San Ysidro Bridge.” Journal of performance of constructed facilities, 20(1), 14-20

Bolton, R., Sikorsky, C., Park, S., Choi, S., and Stubbs, N. (2005) “Modal property changes of a seismically damaged concrete bridge.” Journal of bridge engineering, 10(4), 415-428.

Hu, S.J., Wang, S., and Li, H. (2006) “Cross-modal strain energy method for estimating damage severity.” Journal of engineering mechanics, 132(4), 429-437

Huth, O., Feltrin, G., Maeck, J., Kilic, N., and Motavalli, M., (2005). “Damage identification using modal data: experiences on a prestressed concrete bridge.” Journal of structural engineering, 131(12), 1898-1910

Newtson, C.M., Johnson, G.P., and Enomoto, B.T. (2006). “Fundamental frequency testing of reinforced concrete beams.” Journal of performance of constructed facilities. 20(2), 196-200

Rens, K.L., Nogueira, C.L., and Transue, D.J. (2005). “Bridge management and nondestructive evaluation.” Journal of performance of constructed facilities, 19(1), 3-16

Taly, N. (1998). “Design of modern highway bridges”. McGraw-Hill, New York

Wang, X., Kangas, S., Padur, D., Liu, L., Swanson, J.A., Helmicki, A.J., and Hunt, V.J. (2005). “Overview of a modal-based condition assessment procedure.” Journal of bridge engineering, 10(4), 460-467

Xia, P.Q., and Brownjohn, J.M.W. (2004)“Bridge structural condition assessment using systematically validated finite-element model.” Journal of bridge engineering, 9(5), 418-423

Zhao, J., and Dewolf, J.T. (1999) “Sensitivity study for vibrational parameters used in damage detection.” Journal of structural engineering, 125(4), 410-416.

APPENDIX A - INFLUENCE COEFFICIENTS

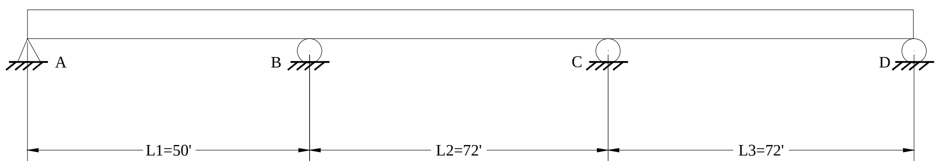

Unit load at		MOMENTS/PL																				
		SPAN 1											SPAN 2									
		A	.1	.2	.3	.4	.5	.6	.7	.8	.9	B	.1	.2	.3	.4	.5	.6	.7	.8	.9	C
	A	0	0	0	0	0	0	0	0	0	0	0	0	0	0	0	0	0	0	0	0	0
SPAN 1	.1	0	.0874	.0747	.0621	.0494	.0368	.0242	.0115	-.0011	-.0138	-.0264	-.0231	-.0198	-.0165	-.0132	-.0099	-.0066	-.0033	.0000	.0033	.0066
	.2	0	.0749	.1498	.1246	.0995	.0744	.0493	.0242	-.0010	-.0261	-.0512	-.0448	-.0384	-.0320	-.0256	-.0192	-.0128	-.0064	.0000	.0064	.0128
	.3	0	.0627	.1254	.1882	.1509	.1136	.0763	.0390	.0018	-.0355	-.0728	-.0637	-.0546	-.0455	-.0364	-.0273	-.0182	-.0091	.0000	.0091	.0182
	.4	0	.0510	.1021	.1531	.2042	.1552	.1062	.0573	.0083	-.0406	-.0896	-.0784	-.0672	-.0560	-.0448	-.0336	-.0224	-.0112	.0000	.0112	.0224
	.5	0	.0400	.0800	.1200	.1600	.2000	.1400	.0800	.0200	-.0400	-.1000	-.0875	-.0750	-.0625	-.0500	-.0375	-.0250	-.0125	.0000	.0125	.0250
	.6	0	.0298	.0595	.0893	.1190	.1488	.1786	.1084	.0381	-.0322	-.1024	-.0896	-.0768	-.0640	-.0512	-.0384	-.0256	-.0128	.0000	.0128	.0256
	.7	0	.0205	.0410	.0614	.0819	.1024	.1229	.1434	.0638	-.0157	-.0952	-.0833	-.0714	-.0595	-.0476	-.0357	-.0238	-.0119	.0000	.0119	.0238
	.8	0	.0123	.0246	.0370	.0493	.0616	.0739	.0862	.0986	.0109	-.0768	-.0672	-.0576	-.0480	-.0384	-.0288	-.0192	-.0096	.0000	.0096	.0192
	.9	0	.0029	.0058	.0088	.0218	.0272	.0326	.0381	.0435	.0490	-.0456	-.0399	-.0342	-.0285	-.0228	-.0171	-.0114	-.0057	.0000	.0057	.0114
	B	0	0	0	0	0	0	0	0	0	0	0	0	0	0	0	0	0	0	0	0	0
SPAN 2	.1	0	-.0039	-.0078	-.0117	-.0156	-.0195	-.0234	-.0273	-.0312	-.0351	-.0390	.0534	.0458	.0382	.0306	.0230	.0154	.0073	.0002	-.0074	-.0150
	.2	0	-.0064	-.0128	-.0192	-.0256	-.0320	-.0384	-.0448	-.0512	-.0576	-.0640	.0192	.1024	.0856	.0688	.0520	.0352	.0184	.0016	-.0152	-.0320
	.3	0	-.0077	-.0154	-.0231	-.0308	-.0385	-.0462	-.0539	-.0616	-.0639	-.0770	-.0042	.0686	.1414	.1142	.0870	.0598	.0326	.0054	-.0218	-.0490
	.4	0	-.0080	-.0160	-.0240	-.0320	-.0400	-.0480	-.0560	-.0640	-.0720	-.0800	-.0184	.0432	.1048	.1664	.1280	.0896	.0512	.0128	-.0256	-.0640
	.5	0	-.0075	-.0150	-.0225	-.0300	-.0375	-.0450	-.0525	-.0600	-.0675	-.0750	-.0250	.0250	.0750	.1250	.1750	.1250	.0750	.0250	-.0250	-.0750
	.6	0	-.0064	-.0128	-.0192	-.0256	-.0320	-.0384	-.0448	-.0512	-.0576	-.0640	-.0256	.0128	.0512	.0896	.1280	.1664	.1048	.0432	-.0184	-.0800
	.7	0	-.0049	-.0098	-.0147	-.0196	-.0245	-.0294	-.0343	-.0392	-.0441	-.0490	-.0218	.0054	.0326	.0598	.0870	.1142	.1414	.0686	-.0042	-.0770
	.8	0	-.0032	-.0064	-.0096	-.0128	-.0160	-.0192	-.0224	-.0256	-.0288	-.0320	-.0152	.0016	.0184	.0352	.0520	.0688	.0856	.1024	.0192	-.0640
	.9	0	-.0015	-.0030	-.0045	-.0060	-.0075	-.0090	-.0105	-.0120	-.0135	-.0150	-.0074	.0002	.0078	.0154	.0230	.0306	.0382	.0458	.0534	-.0390
	C	0	0	0	0	0	0	0	0	0	0	0	0	0	0	0	0	0	0	0	0	0
SPAN 3	.1	0	.0011	.0023	.0034	.0046	.0057	.0068	.0080	.0091	.0103	.0114	.0057	.0000	-.0057	-.0114	-.0171	-.0228	-.0285	-.0342	-.0399	-.0456
	.2	0	.0019	.0038	.0058	.0077	.0096	.0115	.0134	.0154	.0173	.0192	.0096	.0000	-.0096	-.0192	-.0288	-.0384	-.0480	-.0576	-.0672	-.0768
	.3	0	.0024	.0048	.0071	.0095	.0119	.0143	.0167	.0190	.0214	.0238	.0119	.0000	-.0119	-.0238	-.0357	-.0476	-.0595	-.0714	-.0833	-.0952
	.4	0	.0026	.0051	.0077	.0102	.0128	.0154	.0179	.0205	.0230	.0256	.0128	.0000	-.0128	-.0256	-.0384	-.0512	-.0640	-.0768	-.0896	-.1024
	.5	0	.0025	.0050	.0075	.0100	.0125	.0150	.0175	.0200	.0225	.0250	.0125	.0000	-.0125	-.0250	-.0375	-.0500	-.0625	-.0750	-.0875	-.1000
	.6	0	.0022	.0045	.0067	.0090	.0112	.0134	.0157	.0179	.0202	.0224	.0112	.0000	-.0112	-.0224	-.0336	-.0448	-.0560	-.0672	-.0784	-.0896
	.7	0	.0018	.0036	.0055	.0073	.0091	.0109	.0127	.0146	.0164	.0182	.0091	.0000	-.0091	-.0182	-.0273	-.0364	-.0455	-.0546	-.0637	-.0728
	.8	0	.0013	.0026	.0038	.0051	.0064	.0077	.0090	.0102	.0115	.0128	.0064	.0000	-.0064	-.0128	-.0192	-.0256	-.0320	-.0384	-.0448	-.0512
	.9	0	.0007	.0013	.0020	.0026	.0033	.0040	.0046	.0053	.0059	.0066	.0033	.0000	-.0033	-.0066	-.0099	-.0132	-.0165	-.0198	-.0231	-.0264
	D	0	0	0	0	0	0	0	0	0	0	0	0	0	0	0	0	0	0	0	0	0
+ Area		0	.0400	.0700	.0900	.1000	.1000	.0900	.0700	.0402	.0204	.0167	.0152	.0300	.0550	.0700	.0750	.0700	.0550	.0300	.0152	.0167
– Area		0	-.0050	-.0100	-.0150	-.0200	-.0250	-.0300	-.0350	-.0402	-.0654	-.1167	-.0702	-.0500	-.0500	-.0500	-.0500	-.0500	-.0500	-.0500	-.0702	-.1167
Total Area		0	.0350	.0600	.0750	.0800	.0750	.0600	.0350	.0000	-.0450	-.1000	-.0550	-.0200	.0050	.0200	.0250	.0200	.0050	-.0200	-.0550	-.1000

Unit load at		REACTIONS/P				SHEARS/P					
		R_A	R_B	R_C	R_D	V_{AB}	V_{BA}	V_{BC}	V_{CB}	V_{CD}	V_{DC}
SPAN 1	A	1.0	0	0	0	1.0	0	0	0	0	0
	.1	.8736	.1594	-.0396	.0066	.8736	-.1264	.0330	.0330	-.0066	-.0066
	.2	.7488	.3152	-.0768	.0128	.7488	-.2512	.0640	.0640	-.0128	-.0128
	.3	.6272	.4638	-.1092	.0182	.6272	-.3728	.0910	.0910	-.0182	-.0182
	.4	.5104	.6016	-.1344	.0224	.5104	-.4896	.1120	.1120	-.0224	-.0224
	.5	.4000	.7250	-.1500	.0250	.4000	-.6000	.1250	.1250	-.0250	-.0250
	.6	.2976	.8304	-.1536	.0256	.2976	-.7024	.1280	.1280	-.0256	-.0256
	.7	.2048	.9142	-.1428	.0238	.2048	-.7952	.1190	.1190	-.0238	-.0238
	.8	.1232	.9728	-.1152	.0192	.1232	-.8768	.0960	.0960	-.0192	-.0192
	.9	.0544	1.0026	-.0684	.0114	.0544	-.9456	.0570	.0570	-.0114	-.0114
	B	0	1.0	0	0	0	-1.0 / 0	0 / 1.0	0	0	0
SPAN 2	.1	-.0390	.9630	.0910	-.0150	-.0390	-.0390	.9240	-.0760	.0150	.0150
	.2	-.0640	.8960	.2000	-.0320	-.0640	-.0640	.8320	-.1680	.0320	.0320
	.3	-.0770	.8050	.3210	-.0490	-.0770	-.0770	.7280	-.2720	.0490	.0490
	.4	-.0800	.6960	.4480	-.0640	-.0800	-.0800	.6160	-.3840	.0640	.0640
	.5	-.0750	.5750	.5750	-.0750	-.0750	-.0750	.5000	-.5000	.0750	.0750
	.6	-.0640	.4480	.6960	-.0800	-.0640	-.0640	.3840	-.6160	.0800	.0800
	.7	-.0490	.3210	.8050	-.0770	-.0490	-.0490	.2720	-.7280	.0770	.0770
	.8	-.0320	.2000	.8960	-.0640	-.0320	-.0320	.1680	-.8320	.0640	.0640
	.9	-.0150	.0910	.9630	-.0390	-.0150	-.0150	.0760	-.9240	.0390	.0390
	C	0	0	1.0	0	0	0	0	-1.0 / 0	0 / 1.0	0
SPAN 3	.1	.0114	-.0684	1.0026	.0544	.0114	.0114	-.0570	-.0570	.9456	-.0544
	.2	.0192	-.1152	.9728	.1232	.0192	.0192	-.0960	-.0960	.8763	-.1232
	.3	.0238	-.1428	.9142	.2048	.0238	.0238	-.1190	-.1190	.7952	-.2048
	.4	.0256	-.1536	.8304	.2976	.0256	.0256	-.1280	-.1280	.7024	-.2976
	.5	.0250	-.1500	.7250	.4000	.0250	.0250	-.1250	-.1250	.6000	-.4000
	.6	.0224	-.1344	.6016	.5104	.0224	.0224	-.1120	-.1120	.4896	-.5104
	.7	.0182	-.1092	.4638	.6272	.0182	.0182	-.0910	-.0910	.3728	-.6272
	.8	.0128	-.0768	.3152	.7488	.0128	.0128	-.0640	-.0640	.2512	-.7488
	.9	.0066	-.0396	.1394	.8736	.0066	.0066	-.0330	-.0330	.1264	-.8736
	D	0	0	0	1.0	0	0	0	0	0	-1.0
+ Area		.4500	1.2000	1.2000	.4500	.4500	.0167	.5833	.0833	.6167	.0500
- Area		-.0500	-.1000	-.1000	-.0500	-.0500	-.6167	-.0833	-.5833	-.0167	-.4500
Total Area		.4000	1.1000	1.1000	.4000	.4000	-.6000	.5000	-.5000	.6000	-.4000

APPENDIX B - CRACK TESTS AND VISUAL INSPECTION

Crack Tests Performed on Bridge in Meade County

Initial Rading: Girder A

Crackmeter Number	Relative Position of the Crackmeters on the Girder	Orientiation of the Crackmeters	June, 2004: Condition (3) minus Condition (1) (inches)	June, 2004: Condition (3) minus Condition (2) (inches)	May, 2006: Condition (3) minus Condition (1) (inches)	May, 2006: Condition (3) minus Condition (2) (inches)
1	West Side	Vertical	0.0043056	-0.0028704	0.001794	-0.00295682
2	Bottom	Longitudinal	0.0027195	-0.0023569	0.001664522	-0.00375498
3	East Side	Vertical	0.0023556	-0.0012684	0.002278578	-0.00533316

Initial Rading: Girder B

Crackmeter Number	Relative Position of the Crackmeters on the Girder	Orientiation of the Crackmeters	June, 2004: Condition (3) minus Condition (1) (inches)	June, 2004: Condition (3) minus Condition (2) (inches)	May, 2006: Condition (3) minus Condition (1) (inches)	May, 2006: Condition (3) minus Condition (2) (inches)
1	East Side	Horizontal	-0.0001814	-0.0001814	0.002997838	-0.00819928
2		Vertical	0.0052258	-0.0057664	-0.000502671	0.00010884
3	Bottom	Longitudinal	0.004693	-0.005415	0.002936245	**-0.0070746**
4	West Side	Horizontal	-0.0001802	0.0000000	-0.000107904	0.00019954
5		Vertical	0.0052316	-0.0057728	0.002954049	-0.0064397

Note: Condition(1): Front Wheel over the Column (FWOCol) Condition(2): Rear Wheel over the Crack (RWOC)
Condition(3): No Load (NL)

APPENDIX C - FIELD INSPECTION DOCUMENTS

Notes: ***Bridge in Meade County***

1. Visual inspection on June 1, 2004
2. Additional shear cracks were found in Girder A of Span 2 at the same location as the cracks in Girder B.
3. Additional shear crack were also found in Girders A & B in Span 27
4. Installation of gages (temp. 75 ^{o}F) on June 2, 2004

2

4.2. Temperature Correction

The Model 4420 Vibrating Wire Crackmeters have a small coefficient of thermal expansion so in many cases correction may not be necessary. However, if maximum accuracy is desired or the temperature changes are extreme (>10° C) corrections may be applied. The temperature coefficient of the mass or member to which the Crackmeter is attached should also be taken into account. By correcting the transducer for temperature changes the temperature coefficient of the mass or member may be distinguished. The following equation applies;

$$\mathbf{D}_{\mathbf{corrected}} = ((\mathbf{R}_1 - \mathbf{R}_0) \times \underset{G}{\mathbf{C}}) + ((\overset{\Delta T}{\mathbf{T}_1 - \mathbf{T}_0}) \times \mathbf{K})$$

<u>Equation 3 - Thermally Corrected Deformation Calculation</u>

Where; R_1 is the current reading.
R_0 is the initial reading.
C is the calibration factor.
T_1 is the current temperature.
T_0 is the initial temperature.
K is the thermal coefficient (see Equation 4).

3

Tests have determined that the thermal coefficient, K, changes with the position of the transducer shaft. Hence, the first step in the temperature correction process is determination of the proper thermal coefficient based on the following equation;

$$\mathbf{K = ((R_1 \times M) + B) \times C}$$

G

Equation 4 - Thermal Coefficient Calculation

Where; R_1 is the current reading.
M is the multiplier from Table 4.
B is the constant from Table 4.
C is the calibration factor from the supplied calibration sheet.

Model:	4420-12 mm 4420-0.5"	4420-25 mm 4420-1"	4420-50 mm 4420-2"	4420-100 mm 4420-4"	4420-150 mm 4420-6"
Multiplier (M):	0.000295	0.000301	0.000330	0.000192	0.000216
Constant (B):	1.724	0.911	0.415	0.669	0.491

Table 4 - Thermal Coefficient Calculation Constants

Consider the following example using a Model 4420-25 mm Crackmeter;

R_0 = *4773 digits*
R_1 = *4589 digits*
$T_0 = 20.3°\,C$
$T_1 = 32.9°\,C$
6 C = *0.00555 mm/digit*
$K = (((4589 \times 0.000301) + 0.911) \times 0.00555) = 0.0127$
$D_{corrected} = ((R_1 - R_0) \times C) + (((T_1 - T_0) \times K)$
$D_{corrected} = ((4589 - 4773) \times 0.00555) + (((32.9 - 20.3) \times 0.0127)$
$D_{corrected} = (-184 \times 0.00555) + 0.160$
$D_{corrected} = -1.021 + 0.160$
$D_{corrected} = -0.861$ *mm*

2°c Temp. change

example: $(T_1 - T_0) \times K = 2°c \times 0.0127$

$= 0.0254$ mm

$= 0.00254$ cm ← insignificant

Sample Calculations

Thermally corrected deformation calculation:

$D_{corrected} = ((R_1 - R_0) \times G) + ((T_1 - T_0) \times K)$

R_1 is the current reading
R_0 is the initial reading
G is the calibration factor from the supplied calibration sheet
T_1 is the current temperature
T_0 is the initial temperature
K is the thermal coefficient

$K = ((R_1 \times M) + B) \times G$

M is the multiplier, 0.000301
B is the constant, 0.911

$R_1 = 4742$
$R_0 = 4743$
$G = 0.0001814$ (inches / digit)
$T_1 = 23.0\ ^{o}C$
$T_0 = 23.0\ ^{o}C$

$K = (((4742 \times 0.000301) + 0.911) \times 0.0001814)$
$= 0.000424175$ inches

$D_{corrected} = ((4742 - 4743) \times 0.0001814) + (((23\text{-- } - 23\ ) \times 0.000424175)$
$= -0.0001814$ inch.

Meade Bridge

2-Jun-04

Initial Readings:	Girder B
Mark II Snooper:	54,000 GVW
Air Temperature:	77 °F

Table: Crack Tests Performed on Bridge in Meade County

Crackmeter Number	Relative Positions of the Crackmeters on the Girder	Orientation of the Crackmeters	Types of Model Used in the Crack Test	Crackmeter Temperature	Front Wheel over the Column (FWOCol) (1)	Rear Wheel over the Crack (RWOC) (2)	No Load (NL) (3)	Condition (3) minus Condition (1) (3) - (1)	Condition (3) minus Condition (2) (3) - (2)
1	East Side	Horizontal	VWSG	23.0 °C	4743	4743	4742	-1	-1
2		Vertical	VWSG	22.7 °C	4772	4833	4801	29	-32
		Horizontal	Whit		0.0572	0.0572	0.0573	0.0001	0.0001
		Vertical	Whit		0.0569	0.0643	0.0638	0.0069	-0.0005
3	Bottom	Longitudinal	VWSG	22.6 °C	4765	4821	4791	26	-30
		Longitudinal	Whit		0.0521	0.0626	0.0576	0.0055	-0.0050
4	West Side	Horizontal	VWSG	22.6 °C	4673	4672	4672	-1	0
5		Vertical	VWSG	22.5 °C	4859	4920	4888	29	-32
		Horizontal	Whit		0.0177	0.0176	0.0177	0.0000	0.0001
		Vertical	Whit		0.0537	0.0630	0.0588	0.0051	-0.0042

VWSG: Model 4420 Crackmeter
Model GK-403 vibrating wire readout box

Whit: Whittemore Gage

Meade Bridge

2-Jun-04

Initial Readings: Girder B
Mark II Snooper: 54,000 GVW
Air Temperature: 77 °F

Table: Crack Tests Performed on Bridge in Meade County

Crackmeter Number	Relative Positions of the Crackmeters on the Girder	Orientation of the Crackmeters	Types of Model Used in the Crack Test	Crackmeter Temperature	Front Wheel over the Column (FWOCol) (1)	Rear Wheel over the Crack (RWOC) (2)	No Load (NL) (3)	Condition (3) minus Condition (1) (inches) (3) - (1)	Condition (3) minus Condition (2) (inches) (3) - (2)
1	East Side	Horizontal	VWSG	23.0 °C	4743	4743	4742	-0.0001814	-0.0001814
2		Vertical	VWSG	22.7 °C	4772	4833	4801	0.0052258	-0.0057664
3	Bottom	Longitudinal	VWSG	22.6 °C	4765	4821	4791	0.0046930	-0.0054150
4	West Side	Horizontal	VWSG	22.6 °C	4673	4672	4672	-0.0001802	0.0000000
5		Vertical	VWSG	22.5 °C	4859	4920	4888	0.0052316	-0.0057728

VWSG: Model 4420 Crackmeter
Model GK-403 vibrating wire readout box

2/1

Meade Bridge

2-Jun-04

Initial Readings: Girder B
Mark II Snooper: 54,000 GVW
Air Temperature: 77 °F

Table: Crack Tests Performed on Bridge in Meade County

Crackmeter Number	Relative Positions of the Crackmeters on the Girder	Orientation of the Crackmeters	Types of Model Used in the Crack Test	Crackmeter Temperature	Front Wheel over the Column (FWOCol) (1)	Rear Wheel over the Crack (RWOC) (2)	No Load (NL) (3)	Condition (3) minus Condition (1) (inches) (3) - (1)	Condition (3) minus Condition (2) (inches) (3) - (2)
1	East Side	Horizontal	VWSG	23.0 °C	4743	4743	4742	-0.0001814	-0.0001814
2		Vertical	VWSG	22.7 °C	4772	4833	4801	0.0052258	-0.0057664
3	Bottom	Longitudinal	VWSG	22.6 °C	4765	4821	4791	0.0046930	-0.0054150
4	West Side	Horizontal	VWSG	22.6 °C	4673	4672	4672	-0.0001802	0.0000000
5		Vertical	VWSG	22.5 °C	4859	4920	4888	0.0052316	-0.0057728

VWSG: Model 4420 Crackmeter
Model GK-403 vibrating wire readout box

Crack Test \ Meade County \ Meade Bridge – V1

G (inches/digit)	(3) - (1) K (inches)	$D_{corrected}$ (inches)	(3) - (2) $D_{corrected}$ (inches)
0.0001814	0.00042418	-0.0001814	-0.0001814
0.0001802	0.00042457	0.0052258	-0.0057664
0.0001805	0.00042473	0.0046930	-0.0054150
0.0001802	0.00041757	-0.0001802	0.0000000
0.0001804	0.00042976	0.0052316	-0.0057728

Meade Bridge

June 2, 2004

"Span 2 Girder B"

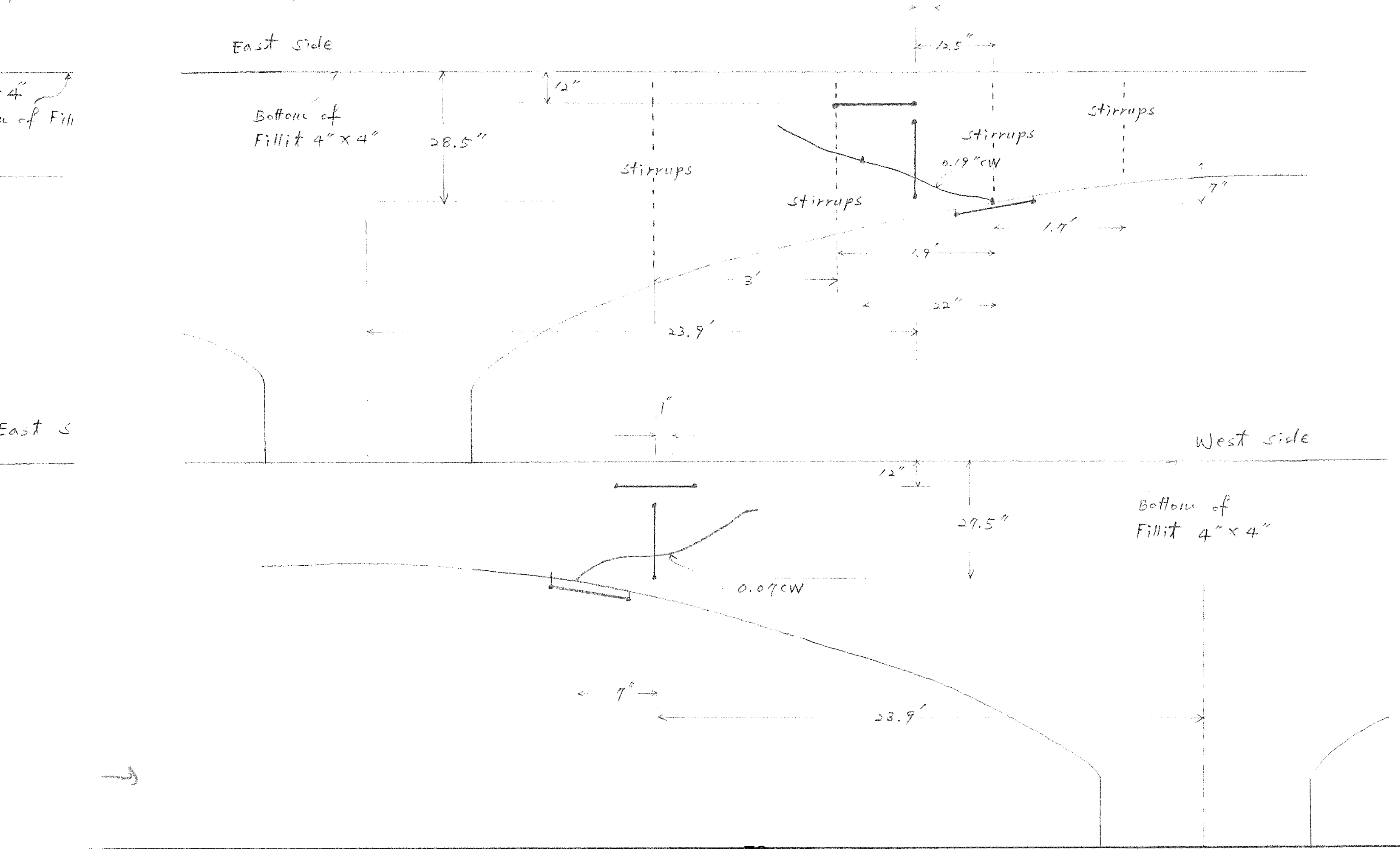

3/6

"Span 2 Girder A"

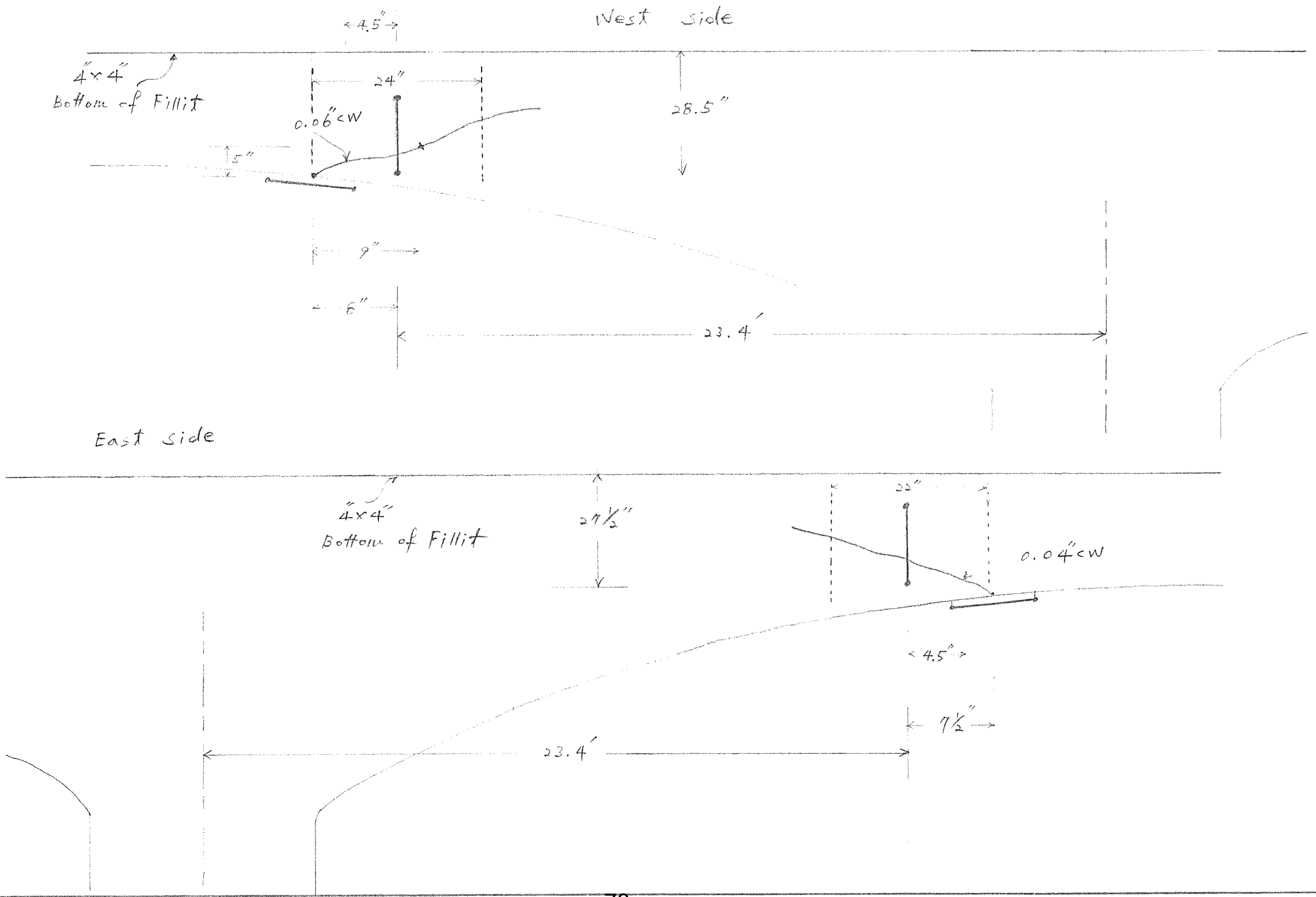

Meade Bridge

June 3, 04

5/6

Meade Bridge

3-Jun-04

Initial Readings: Girder A
Mark II Snooper: 54,000 GVW
Air Temperature: 74.5 °F

Table: Crack Tests Performed on Bridge in Meade County

Crackmeter Number	Relative Positions of the Crackmeters on the Girder	Orientiation of the Crackmeters	Types of Model Used in the Crack Test	Crackmeter Temperature	Front Wheel over the Column (FWOCol) (1)	Rear Wheel over the Crack (RWOC) (2)	No Load (NL) (3)	Condition (3) minus Condition (1) (3) - (1)	Condition (3) minus Condition (2) (3) - (2)
1	West Side	Vertical Vertical	VWSG Whit	24.0 °C	4558 0.0542	4598 0.0642	4582 0.0643	24 0.0101	-16 0.0001
2	Bottom	Longitudinal Longitudinal	VWSG Whit	23.4 °C	4819 0.0193	4847 0.0135	4834 0.0220	15 0.0027	-13 0.0085
3	East Side	Vertical Vertical	VWSG Whit	23.3 °C	4747 0.0642	4767 0.0688	4760 0.0575	13 -0.0067	-7 -0.0113

VWSG: Model 4420 Crackmeter
Model GK-403 Vibrating Wire Readout Box

Whit: Whittemore Gage

Meade Bridge
3-Jun-04

Initial Readings: Girder A
Mark II Snooper: 54,000 GVW
Air Temperature: 74.5 °F

Table: Crack Tests Performed on Bridge in Meade County

Crackmeter Number	Relative Positions of the Crackmeters on the Girder	Orientiation of the Crackmeters	Types of Model Used in the Crack Test	Crackmeter Temperature	Front Wheel over the Column (FWOCol) (1)	Rear Wheel over the Crack (RWOC) (2)	No Load (NL) (3)	Condition (3) minus Condition (1) (inches) (3) - (1)	Condition (3) minus Condition (2) (inches) (3) - (2)
1	West Side	Vertical	VWSG	24.0 °C	4558	4598	4582	0.0043056	-0.0028704
2	Bottom	Longitudinal	VWSG	23.4 °C	4819	4847	4834	0.0027195	-0.0023569
3	East Side	Vertical	VWSG	23.3 °C	4747	4767	4760	0.0023556	-0.0012684

VWSG: Model 4420 Crackmeter
Model GK-403 Vibrating Wire Readout Box

G (inches/digit)	(3) - (1) K (inches)	$D_{corrected}$ (inches)	(3) - (2) $D_{corrected}$ (inches)
0.0001794	0.0004109	0.0043056	-0.0028704
0.0001813	0.000429	0.0027195	-0.0023569
0.0001812	0.0004247	0.0023556	-0.0012684

Meade Bridge

3-Jun-04

Initial Readings: Girder A
Mark II Snooper: 54,000 GVW
Air Temperature: 74.5 °F

Table: Crack Tests Performed on Bridge in Meade County

Crackmeter Number	Relative Positions of the Crackmeters on the Girder	Orientiation of the Crackmeters	Types of Model Used in the Crack Test	Crackmeter Temperature	Front Wheel over the Column (FWOCol) (1)	Rear Wheel over the Crack (RWOC) (2)	No Load (NL) (3)	Condition (3) minus Condition (1) (inches) (3) - (1)	Condition (3) minus Condition (2) (inches) (3) - (2)
1	West Side	Vertical	VWSG	24.0 °C	4558	4598	4582	0.0043056	-0.0028704
2	Bottom	Longitudinal	VWSG	23.4 °C	4819	4847	4834	0.0027195	-0.0023569
3	East Side	Vertical	VWSG	23.3 °C	4747	4767	4760	0.0023556	-0.0012684

VWSG: Model 4420 Crackmeter
Model GK-403 Vibrating Wire Readout Box

4/6

Meade Bridge Notes

Visual Inspection June 1, 04

Additional Shear Cracks were found in girder A of span 2 at the same location as the Cracks in Girder B.

Additional Shear Cracks were also found in Girders A & B in span 27.

June 2, 04

Installation of gages

Temp 75°

15

Initial Readings — Mark II Snooper 54,000 GVW

Girder B — Air Temp 77°

East Side

				FWO col	RWOC	N.L
1	Horizontal	VWSG	23.0C	4743 µE	4743 µE	4742µE
2	Vertical	VWSG	22.7C	4772 µE	4833µE	4801µE
	Horiz	Whit		572	572	.0573
	Vertical	Whit		569	643	.0638

West Side

4	Horigontal	VWSG	22.6°C	4673µE	4672 µE	4672µE
5	Vertical	VWSC	22.5°C	4859µE	4920µE	4888µE
	Horiz	Whit		.0177	.0176	.0177
	Vertical	Whit		.0537	.0630	.0588

Bottom

3	VWSG		22.6°C	4765	4821 µE	4791 µE
	whit			521	626	.0596

Check 2°C Temp Change

16

Meade Bridge

Span 2 Girder B

June 2, 04

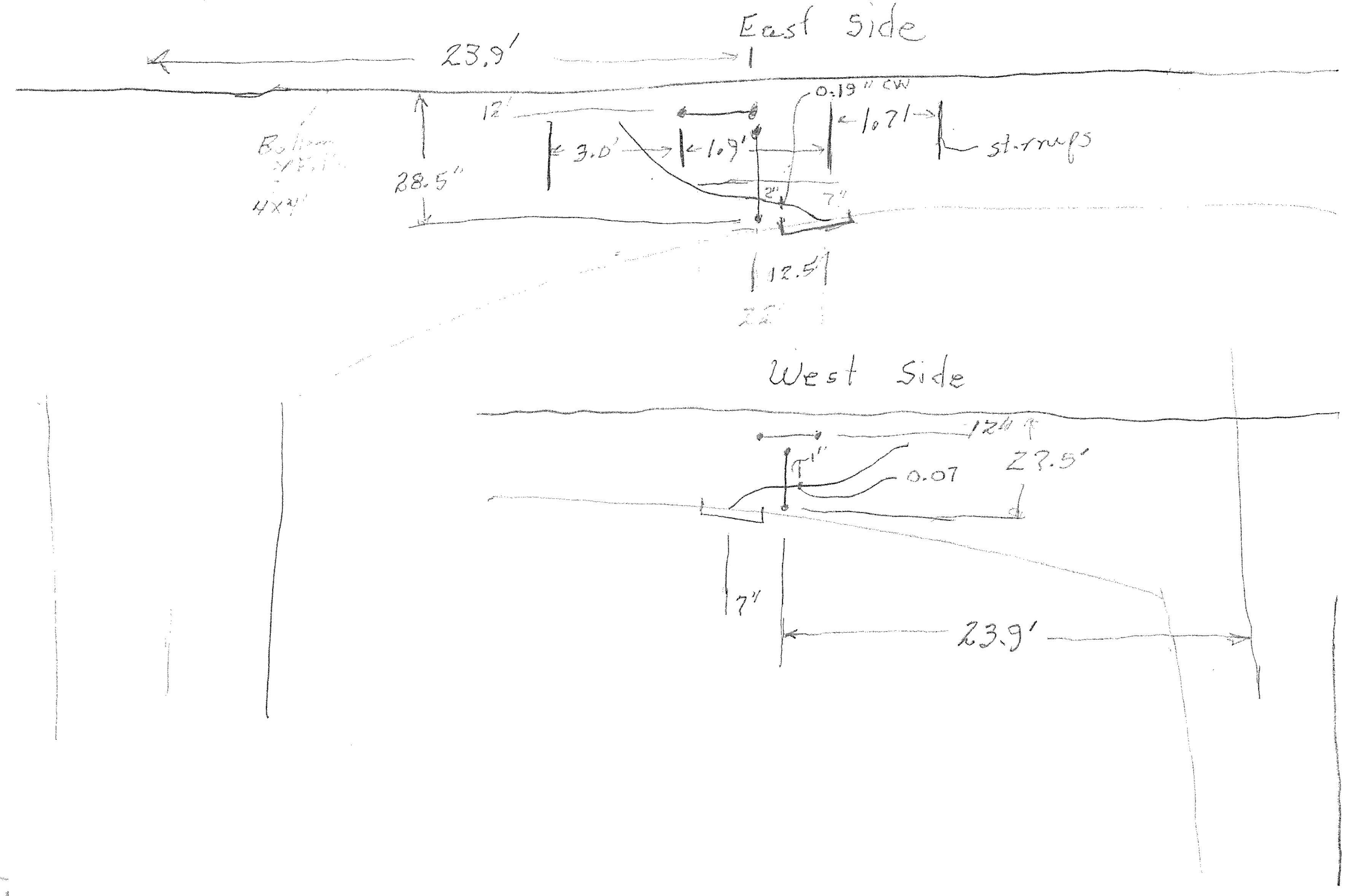

Meade Bridge | | June 3, 04 | 4/

Initail Readings   Mark II Snooper 54,000 GVW

Girder A   Air Temp 74.5°F

West Side				FWOCol	RWOC	N.L.
1	Vertical	VWSG	24.0°C	4558 $\mu\epsilon$	4598	4582
	Vertical	Whit		.0542	.0642	.0643

East Side

3	Vertical	VWSG	23.3°C	4747 $\mu\epsilon$	4767 $\mu\epsilon$	4760 $\mu\epsilon$
	Vertical	Whit		.0642	.0688	.0575

Bottom

2	VWSG	23.4°C	4819 $\mu\epsilon$	4847 $\mu\epsilon$	4834 $\mu\epsilon$
	Whit		.0193	.0135	.0220

18

Meade Bridge

Span 2 Girder A

June 3, 04

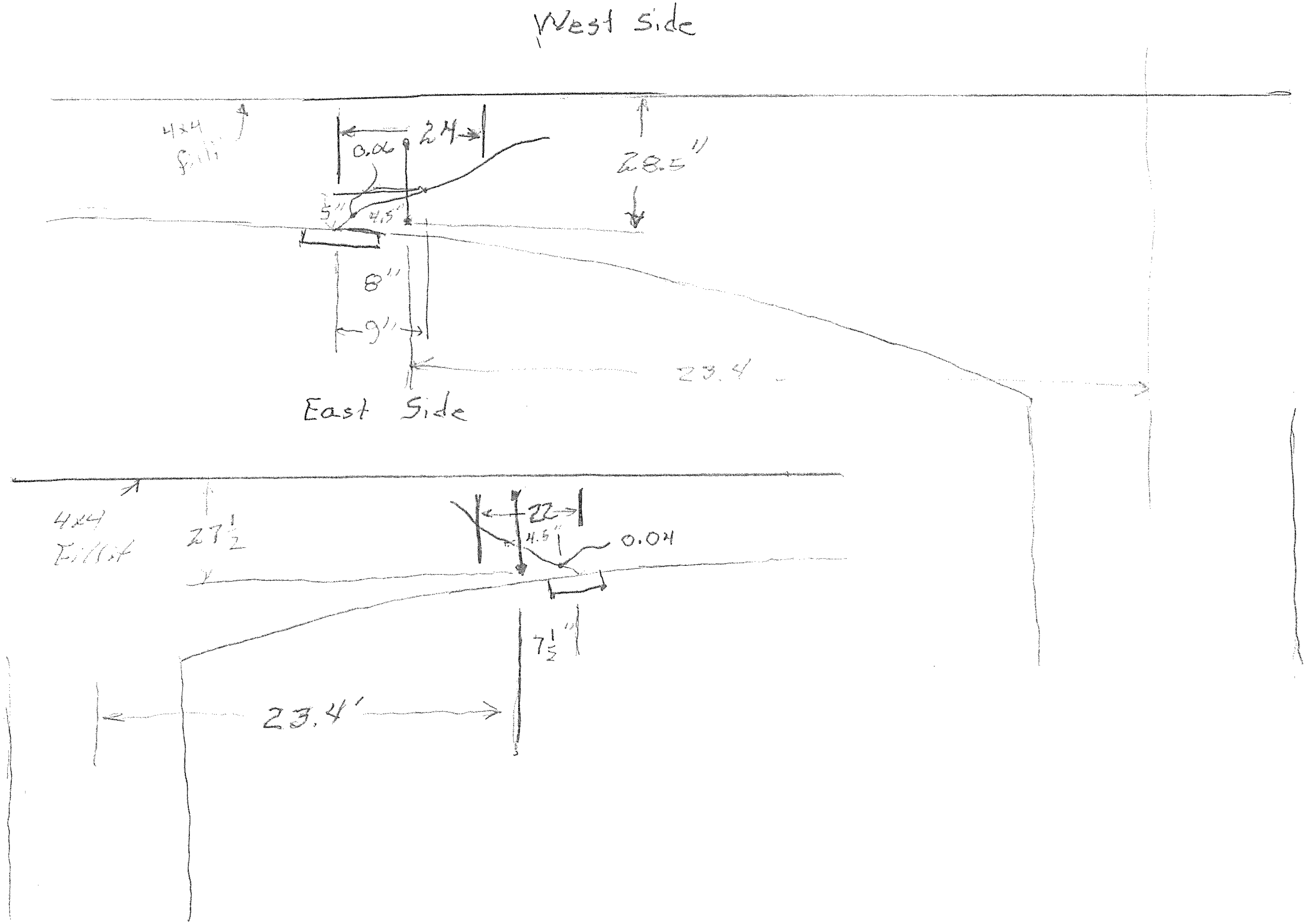

* Snooper Axle Distance :

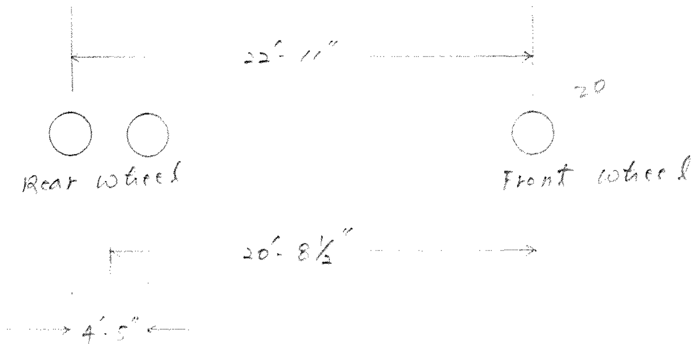

* Front wheel over the Column

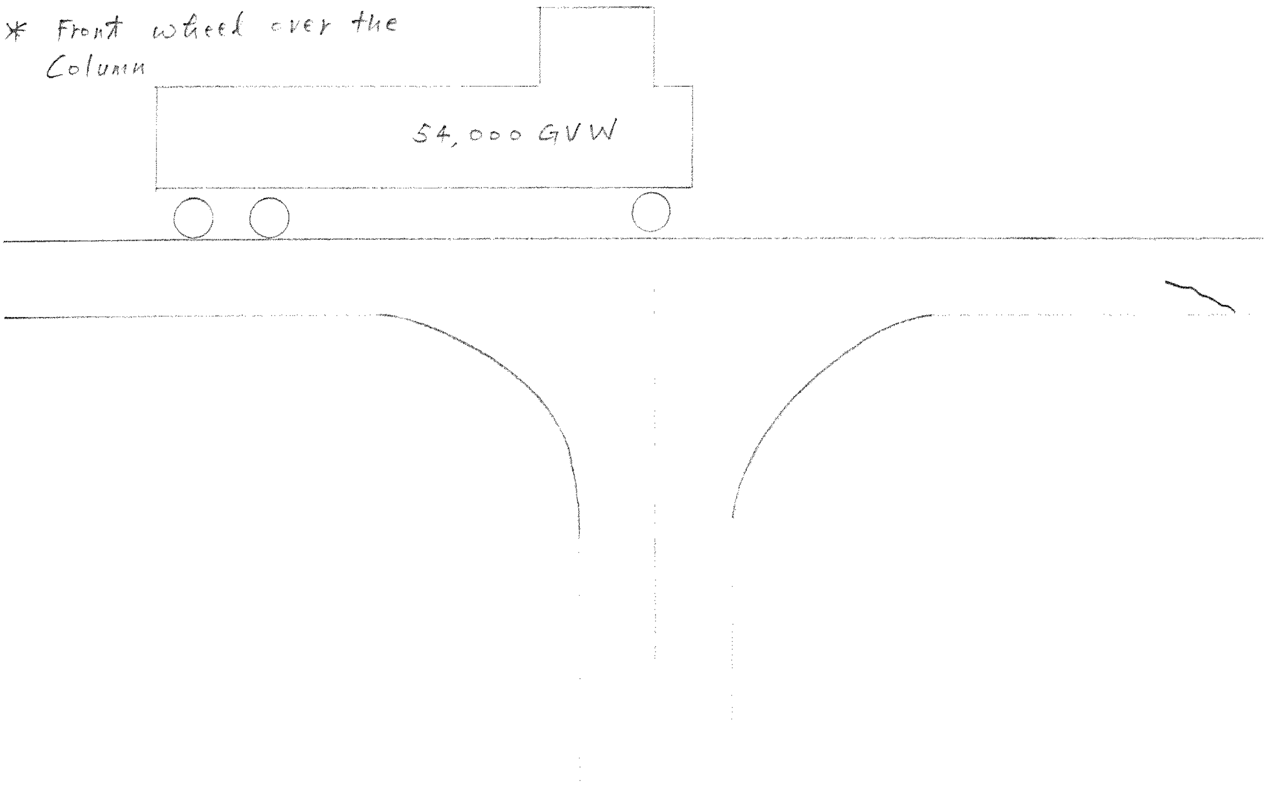

* Rear wheel over the Crack

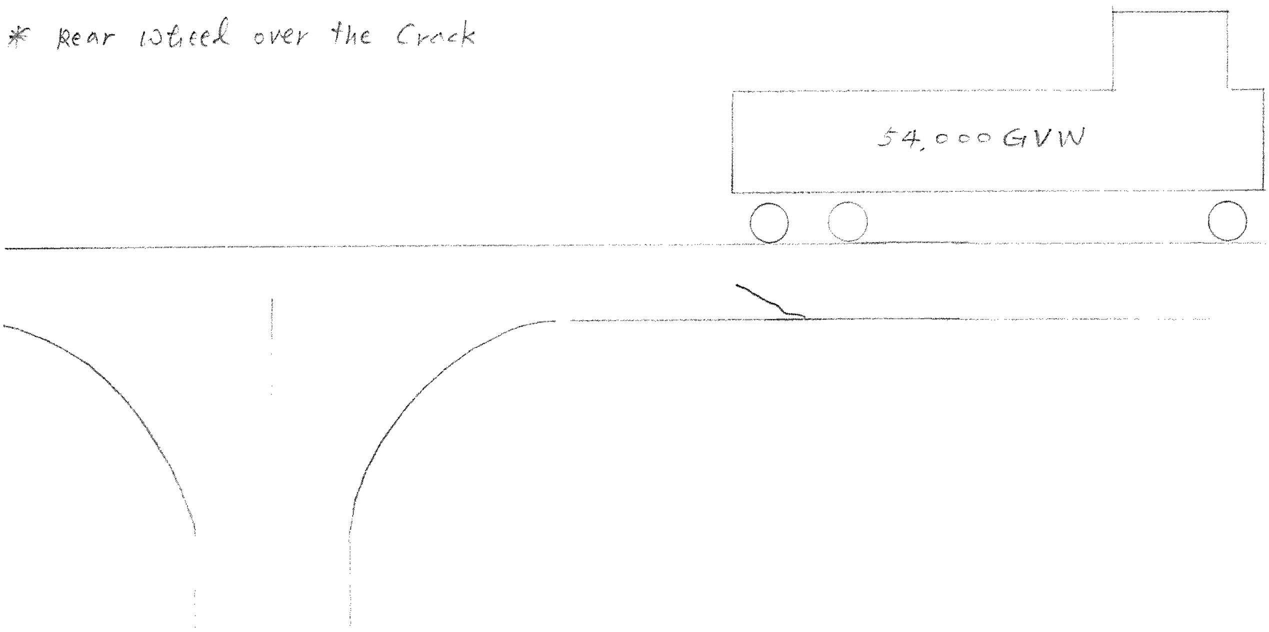

20

MAPQUEST

Send To Printer Back to Map

Liberal KS
US

Notes: OVER VIEW NO MOTEL LOCATION NE PAGE 0

~~8~~7 ROOMS TOTAL

CONF# 66066603

WILL ACCEPT PA'S. DAN HAS ONE

Dave — Snooper axle distance?

Front wheel → farthest back axle — 22'-11"

between rear axles – 4'-5" / 2-2½

Front axle to between rear axles 20'-8½"

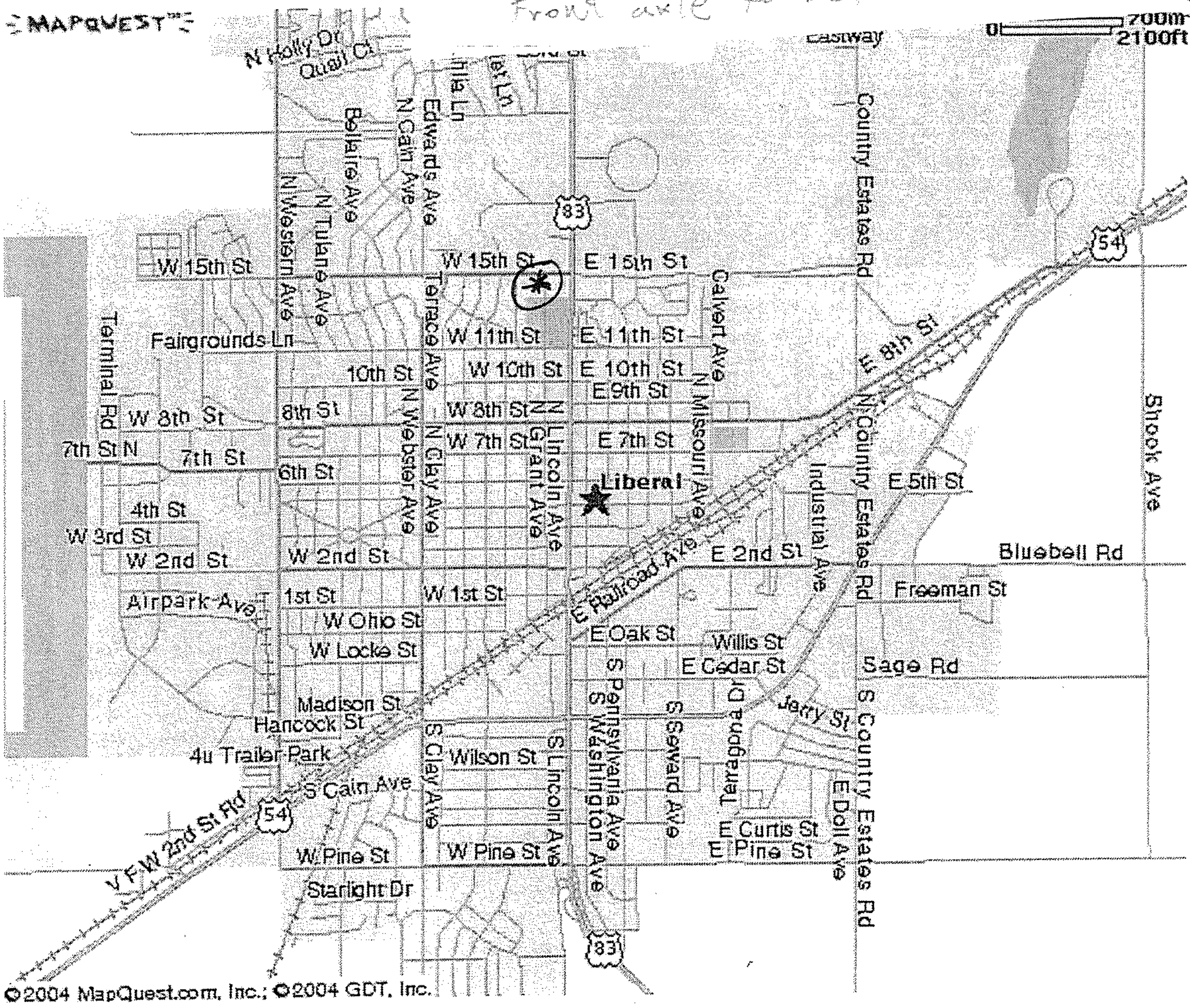

21

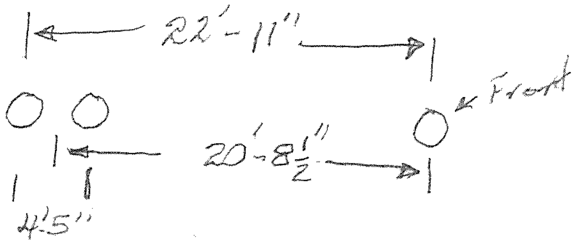
22'-11"
Front
20'-8½"
4'5"

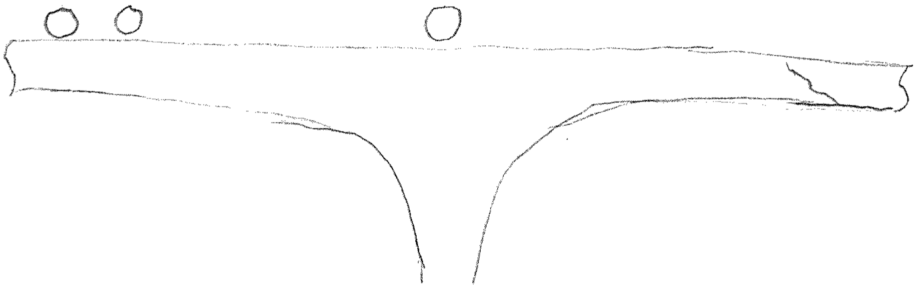

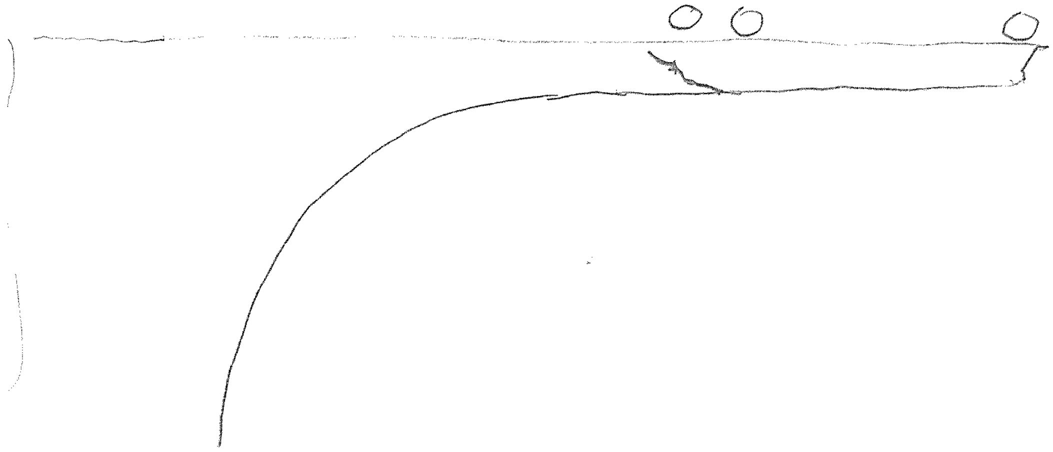

Date: ~~April~~ May, 2006.

Meade Bridge

initial Rading: Girder A
Air Temperature:

Table : Crack Test Performed on Bridge in Meade County

Gauge Number	Location of gauge	No.	Crackme Tempera	No Load (NL) (3)	Front Wheel Over the Column(FWOCol) (1)	Rear Wheel Over the Crack(RWOC) (2)	Condion(3) minus Condition (1) (3)-(1)	Condion(3) minus Condition (2) (3)-(2)	Corrected Deformation (3)-(1)
1	west	04--4535		4878.7	4870.0	4895.0	8.7	-16.3	0.001794
2	bottom	04--4526		4888.7	4880.0	4909.4	8.7	-20.7	0.001664522
3	east	04--4527		4644.5	4632.4	4673.9	12.1	-29.4	0.002278578

initial Rading: Girder B
Air Temperature:

Table : Crack Test Performed on Bridge in Meade County

Gauge Number	Location of gauge	orientation of gauge	No.	Crackmeter Temperature	No Load (NL) (3)	Front Wheel Over the Column(FWOCol) (1)	Rear Wheel Over the Crack(RWOC) (2)	Condion(3) minus Condition (1) (3)-(1)	Condion(3) minus Condition (2) (3)-(2)
1	east	verticle	04--4532		4735.8	4735.3	4735.2	0.5	0.6
2	side	Standard	04--4533		4845.2	4828.2	4890.4	17.0	-45.2
3	bottom	longitudinal	04--4530		4874.0	4857.1	4913.0	16.9	-39.0
4	west	horizontal	04--4528		4668.2	4668.1	4667.1	0.1	1.1
5	side	vertical	04--4529		4894.5	4877.5	4930	17.0	-35.5

N
ω

Corrected Deformation (3)-(2)	K
-0.00295682	0.000431639
-0.00375498	0.00043171
-0.00533316	0.000418191

Corrected Deformation (3)-(1)	Corrected Deformation (3)-(2)	K
-0.000502671	0.00010884	0.000423837
0.002997838	-0.00819928	0.00042981
0.002936245	-0.0070746	0.000431383
-0.000107904	0.00019954	0.000420146
0.002954049	-0.0064397	0.000432502

2.4

Meade Bridge

Girder A

Gage	No	(3) unloaded	(1) Front wheel over the Column FWOCOL Load A	(2) Rear wheel over the crack Rear Wheel O Load B
1	04-4527	22.0 4644.5	4632.4 21.5	4673.9 21.9
2	04-4526	21.3 4888.7	4880.0 21.7	4909.4 20.6
3	04-4535	20.9 4878.7	4870.0 20.7	4895.0 20.7

Whi

1 East — Lost

2 Bottom — Could Not Read Over gage Length

3 West

Girder B

Gage	No	unloaded	Load A	Load B
1 check	04-4532	20.2 4735.8	21.6 4735.3	4735.2 21.8
2	04-4533	21.3 4845.2	4828.2 21.5	4890.4 21.4
3	04-4530	20.8 4874.0	4857.1 21.1	4913.0 21.2
4668.8 4 check	04-4528	20.2 4668.2	4668.1 20.5	4667.1 20.6
5	04-4529	20.1 4894.5	20.4 4877.5	4930.0 20.7

Whi

1 East Vert	overlength		
2 Standard East Side	242		
3 Bottom	overlength		
4 West Horiz Check	-147	-145	-145
5 West Vert	306	292	out of Range

25

DEPARTMENT OF TRANSPORTATION

AD ASTRA PER ASPERA

KANSAS